



# Düzce University Journal of Science & Technology

Research Article

## Theoretical Investigation of the Molecular Properties of the Fluoroaniline and Fluoroanisole Isomers

 Yavuz EKİNCİOĞLU <sup>a,\*</sup>,  Abdullah KEPCEOĞLU <sup>b</sup>

<sup>a</sup> Bayburt University, Department of Opticianry, Bayburt, TÜRKİYE

<sup>b</sup> Koç University Surface Science and Technology Center (KUYTAM), İstanbul, TÜRKİYE

\* Corresponding author's e-mail address: yekincioglu@bayburt.edu.tr

DOI: 10.29130/dubited.1396459

### ABSTRACT

This research paper aims to analyse the molecular properties of fluoroaniline and fluoroanisole isomers through a range of theoretical methods. These methods include optimization of molecular structures, conformational analysis, and calculation of nonlinear optics (NLO) properties, frontier molecular orbital (HOMO-1, HOMO/SOMO, LUMO, LUMO+1) energies, chemical reactivity descriptors (ionization potentials - vertical and adiabatic, electron affinity, chemical hardness, softness, and electronegativity), molecular electrostatic potential (MEP), natural bonding orbital (NBO), and UV-Vis spectra. To achieve this, the density functional theory method with B3LYP functional and 6-311++G (d, p) basis set were used for the calculations. Additionally, the research examines the vertical and adiabatic ionization energy parameters of the molecules by constructing singly charged cation radicals. The outcome of this study provides valuable insights into the molecular properties of fluoroaniline and fluoroanisole isomers, which can be useful in the production of pharmaceuticals and agrochemicals.

**Keywords:** Isomers, FMOs, NLO, MEP, TD-DFT, Ionization energy.

## Floroanilin ve Floroanizol İzomerlerin Moleküler Özelliklerinin Teorik İncelenmesi

### Öz

Bu çalışmada, floroanilin ve floroanizol izomerlerinin moleküler özelliklerini çeşitli teorik yöntemlerle analiz edilmesi amaçlanmaktadır. Bu yöntemler arasında moleküler yapıların optimizasyonu, konformasyon analizi ve doğrusal olmayan optik (NLO) özelliklerin, sınır moleküler orbital (HOMO-1, HOMO/SOMO, LUMO, LUMO+1) enerjilerinin, kimyasal reaktivite tanımlayıcılarının (iyonlaşma potansiyelleri - dikey ve adyabatik, elektron afinitesi, kimyasal sertlik, yumuşaklık ve elektronegatiflik), moleküler elektrostatik potansiyel (MEP), doğal bağ orbital (NBO) ve UV-Vis spektrumlarının hesaplanması bulunmaktadır. Bu hesaplamaları gerçekleştirmek için, yoğunluk fonksiyonel teorisi (YFT) yöntemi B3LYP fonksiyonu ve 6-311++G (d, p) baz seti kullanılmıştır. Ayrıca, araştırmada, moleküllerin dikey ve adyabatik iyonizasyon enerji parametrelerini tek yüklü kation radikalleri oluşturarak incelemektedir. Bu çalışmanın sonuçları, floroanilin ve floroanizol izomerlerinin moleküler özelliklerine dair değerli bilgiler sağlamaktadır ve bu bilgiler, ilaç ve tarım kimyasalları üretiminde faydalı olabilir.

**Anahtar Kelimeler:** İzomerler, FMOs, NLO, MEP, TD-DFT, İyonlaşma Enerjisi

# **I. INTRODUCTION**

Fluoroanilines, namely 2-, 3-, and 4-fluoroaniline, or o-, m-, p-fluoroaniline, are commonly employed in synthesizing pesticides, plant growth regulators, and larger molecules. These chemicals may pose a risk to agricultural workers and other living organisms, prompting researchers to investigate their effects on the microsomal system. The  $^{19}\text{F}$ -NMR method was employed to explore the effects as mentioned earlier [1].

The impact of halogen atoms, such as F, Cl, and Br, bonded to the aniline molecule was examined in relation to the molecule's geometric structure and vibrational frequencies. The  $\pi$ -electrons of the aniline ring to which the halogens are attached were observed to be displaced, with the halogens contributing to this displacement. Moreover, it was determined that para-halogen-aniline molecules contributed less to these electron displacements compared to ortho- and meta-halogen aniline molecules [2].

In addition, the ground state vibrations of the p-fluoroaniline molecule in the IR region and far-IR regions were studied [3, 4].

UV absorption spectra ( $S_1 \leftarrow S_0$  transitions) have also been studied for fluoraniline isomers, and it is reported that no results were observed for the change of molecular geometry between the ground state and the excited state [5]. In contrast, in another study investigating similar properties, the base ( $S_0$ ) and first excited singlet ( $S_1$ ) energy levels of the p-fluoroaniline (4-fluoroaniline) molecule were investigated both experimentally and ab-initio. The  $S_0 \leftarrow S_1$  transitions and the related vibrational bands have been investigated both experimentally by UV-fluorescence excitation and comparatively by DFT methods. It was observed that the minimum potential of the amino group attached to the benzene ring varies between -20 and 20 for the  $S_1$  level depending on the pyramidal structure and dihedral angle [6]. Similarly, the photoelectron spectra of fluoronitrobenzene isomers were analyzed using He(I) and He(II) photoelectron spectroscopy and ab initio methods [7].

Resonance two-photon ionization studies (R2PI) determined that the 0-0 band transition for p-fluoroaniline is at 306.25nm [8]. Similarly, the 0-0 transition for p-fluoroaniline was experimentally observed at 306.20 nm. Additionally, all levels spanning from 306.20 nm down to 287.34 nm were discerned [9].

Adiabatic ionization energy values for the cationic ground state of the p-fluoroaniline molecule were experimentally determined using mass-analyzed threshold ionization (MATI) and two-color resonant two-photon ionization (2CR2PI) methods, and ionization energies and vibrational frequencies of the ground state and cationic state were also calculated using the DFT method. They were measured experimentally at  $62543\text{ cm}^{-1}$  (7.754 eV) with MATI and  $62550\text{ cm}^{-1}$  (7.755 eV) with 2CR2PI. In calculations using the DFT method and B3LYP/6-311+G\*\* basis sets, this value was calculated as  $61084\text{ cm}^{-1}$  (7.573 eV), a difference of 2.3% [10]. A similar study was performed for o-fluoroaniline and the ionization energy was found to be  $63644 \pm 5\text{ cm}^{-1}$  ( $7.8904 \pm 0.0006\text{ eV}$ ) [11]. For the o-fluoroaniline molecule, this value was found to be  $64159 \pm 5\text{ cm}^{-1}$  ( $7.9542 \pm 0.0006\text{ eV}$ ) [12].

Proton affinities of various MALDI matrices were determined by electrospray ionization (ESI) employing the kinetic method. P-fluoroaniline and aniline-derived chemicals served as a reference compounds for this purpose [13].

Ionization of fluoraniline isomers utilizing the atmospheric-pressure photoionization-ion mobility spectrometry-mass spectrometry (APPI-IMS-MS) method (ionization was performed with a krypton lamp) revealed the presence of product ions  $M^{\bullet+}$  (100%),  $(M+18)^{\bullet+}$  (79%). Additionally peaks indicative of (water molecule + parent molecule) were predominantly observed in the mass spectrum [14].

Due to advancements in computer technology and quantum chemistry, molecular modeling is becoming more prevalent. Parallel to these improvements, ab initio methods play an important role in explaining

experimental and theoretical findings [15]. One of the most prominent of these methods is density functional theory (DFT), which uses a quantum mechanical modeling methodology to investigate the electronic structure of molecules, their spectroscopic properties, and energy values, all at a low cost [16, 17]. Furthermore, DFT has proven to be an effective research tool for validating or characterizing experimental results [18].

In this investigation, Floraniline, a chemical compound manifesting three distinct isomeric configurations, constitutes the subject under scrutiny. The molecular composition and associated physical and chemical attributes of the respective Floraniline isomers are delineated in Table 1, retrieved from the NIST database.

*Table 1. Structure and properties of fluoroaniline isomers*

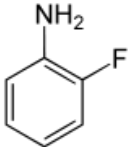
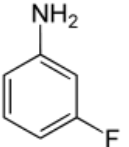
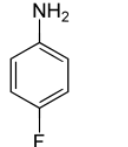
Isomer	<b>o-Fluoroaniline</b> (2-Fluoroaniline)	<b>m-Fluoroaniline</b> (3-Fluoroaniline)	<b>p-Fluoroaniline</b> (4-Fluoroaniline)
Structure			
CAS	348-54-9	372-19-0	371-40-4
Mp °C	-35 °C	-5 °C	-35 °C
Bp °C	182–183 °C	186.3±13.0 °C	182–183 °C
Density g/mL	1.151	1.156	1.173
Refractive Index	1.544	1.542	1.539
Ionization Energy (eV)	8.50 [19]	8.32 [21]	7.9 [22]
	8.18 [20, 21]	8.33 [20]	8.18 [20, 21]

Table 1 delineates the physical properties of fluoraniline isomers, present in a liquid state under ambient conditions, with boiling points approximately at 180°C. The ionization energies of ortho- and meta-isomers are close in proximity, whereas the para-fluoroaniline molecule exhibits a diminished value. Anisole, with the molecular formula C<sub>7</sub>H<sub>8</sub>O, is a versatile molecule utilized in the production of various compounds, including pesticides, medicines, flavourings, and perfumes. The preparation of synthetic anethole, for instance, involves the use of anisole. In terms of reactivity, anisoles exhibit a greater electrophilic aromatic substitution rate than benzene. Furthermore, fluoroanisoles have found extensive application in the production of pharmaceuticals, agricultural tools, and fluorinated medical compounds. Of note, the 4-fluoroanisole isomer has been utilized in the synthesis of a thermally and chemically stable polymer that shows potential for use in optoelectronics, batteries, and sensors [23].

Isomers of molecules play a crucial role in delineating the physical properties associated with the molecular system. Fluoroanisole exhibits three distinct isomers, namely 2-, 3-, and 4-fluoroanisole, designated as o-, m-, and p-fluoroanisole (or ortho-, meta-, para-fluoroanisole). The conformer characteristics of fluoroanisoles have been studied many times in experimental and theoretical studies. Several research groups have studied the conformational properties of anisole molecules by using electron diffraction [24], microwave spectroscopy [25], and high-resolution spectroscopy [26] method experimentally, and ab-initio and DFT [27] computational approaches. The molecular geometry of 2-fluoroanisole has been specifically investigated using FT-IR spectroscopy and quantum chemical methods [25, 27].

The mass analysis threshold ionization spectra of anisole were performed by ionizing four vibrational states and as a result, the adiabatic ionization energies of these species were determined to be 8.23243±0.00062 eV [28]. Similarly, the molecular properties of anisole in the ground state and the first excited state have been investigated using various spectroscopic techniques. As a result, the ionization energy of anisole is presented as 8.20 ± 0.05 eV.

Infrared absorption, Raman scattering, optical absorption, and thermal analysis were studied experimentally and with the DFT (3-21g\*) basis set to assess the vibrations and optical properties. Time-resolved photoluminescence (TR-PL) spectroscopy was used to evaluate both chloroform solutions and film states. The faster PL decays in the thin film are shown to result from both conformer structures and  $\pi$ - $\pi$  stacking interactions among molecules [29].

The vibrational structure of 4-fluoroanisole in its first excited state was investigated by mass-selected resonance-enhanced two-photon ionization spectroscopy and the  $S_1 \leftarrow S_0$  transition of 4-fluoroanisole was found to occur at 4.35792 eV. The vibrational frequencies and optimized molecular geometries of the ground state and cation ground state were determined by DFT calculations. The molecular structures and conformer properties of 2- and 4- fluoroanisole in the gas phase were investigated by electron diffraction techniques alongside quantum chemical calculations [30].

The cation spectra of 2-fluoroanisole and 4-fluoroanisole isomers were obtained using two-colour resonance two-photon mass analysis threshold ionization spectroscopic techniques. The adiabatic ionization energies of these structures were found to be  $8.35083 \pm 0.00062$  eV and  $8.23714 \pm 0.00062$  eV, respectively. Consequently, the positions of the F atom and the OCH<sub>3</sub> group are significantly impact the transition energies and molecular vibrations. The adiabatic ionization energies for the cis and trans states of the 3-fluoroanisole molecule were found to be  $8.41444 \pm 0.00062$  eV and  $8.46862 \pm 0.00062$  eV for the cis and trans states, respectively, using the same spectroscopic techniques. As a result, the localization of the F atom and the OCH<sub>3</sub> group plays a crucial role in influencing both transition energies and molecular vibrations [31].

The proton affinities of 2-, 3- and 4-fluoroanisole molecules were determined via Fourier transform ion cyclotron resonance (FT-ICR) mass spectra. The values obtained were 808 kJ mol<sup>-1</sup> (2-fluoroanisole), 825 kJ mol<sup>-1</sup> (3-fluoroanisole) and 795 kJ mol<sup>-1</sup> (4-fluoroanisole). The experimental data were compared with the proton affinities calculated using ab-initio methods employing the G3, G3(MP2) and MP2(fc)/6-11G(2d,p)//HF/6-31G(d,p) basis sets. As a result of these comparisons, calculations with the G3(MP2) basis set gave the best evaluation in experimental and ab-initio calculations [32]. Comparisons of ionization and appearance potentials of m- and p-X doped anisoles [M - CH<sub>3</sub>] and [M - CH<sub>3</sub>O] revealed that their difference did not exceed approximately 0.20 eV [33].

The standard enthalpies of formation of the three isomers of the fluoroanisole molecule in the liquid phase were compared with experimental and theoretical calculations. As a result, they are ordered at positions  $3 > 4 > 2$  [34].

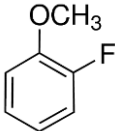
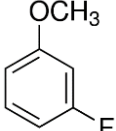
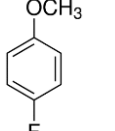
Molecular structure and conformer studies of 4-fluoroanisole and 3,4-difluoroanisole molecules were conducted employing diverse quantum chemical computation methods. It was determined that 4-fluoroanisole possesses solely a singular conformer [35].

The molecular structure and conformer analyses of 2-fluoroanisole were studied using diverse quantum chemical calculation methods. The impact of the fluorine atom introduction to anisole on its conformer and molecular structure were studied. In addition, stereochemical, specifically orbital interaction energies, were analyzed by natural bonding orbital (NBO) analysis [36].

Also, in the literature, jet-cooled laser-induced fluorescence (LIF) excitation, UV-UV cavity combustion and single vibrational level fluorescence (SVLF) spectra of 2-fluoroanisole were measured. The most intense lowest frequency band at 4.53931 eV was determined to mark the onset of the most stable trans conformer. The vibrational band analysis using B3LYP/cc-pVTZ and CIS/6-311G(d,p) levels was conducted via quantum chemical calculations [37].

The chemical under examination in this study is fluoroanisole, which comprises three distinct isomers. The molecular structure along with select physical and chemical properties of fluoroanisole isomers are detailed in Table.2, sourced from the NIST database.

*Table 2. Structure and properties of fluoroanisole isomers*

Isomer	<b>o-Fluoroanisole</b> (2-Fluoroanisole)	<b>m-Fluoroanisole</b> (3-Fluoroanisole)	<b>p-Fluoroanisole</b> (4-Fluoroanisole)
Structure			
CAS	321-28-8	456-49-5	459-60-9
Mw (amu)	126.13	126.13	126.13
Mp °C	-39	-35	-45
Bp °C	154-155	158	157
Density g/mL	1.124	1.104	1.114
Ionization Energy (eV)	8.91 [38] 8.92 [39]	8.41 [40] 8.7 [33]	8.6 [33] 8.79 [38]

As seen in Table.2, fluoroanisole isomers are liquid at room temperature, and their boiling temperatures are approximately ~155 °C. The ionization energies of the o- and p- isomers are close to each other, with a lower value observed in the m-fluoroanisole molecule.

## **II. MATERIAL AND METHODS**

The conformer analysis and theoretical calculations of various properties of Fluoroaniline and Fluoroanisole isomers were performed in this study. The Merck molecular force field (MMFF) in the molecular mechanic method was used to carry out the conformer analysis by the Spartan 08 package program [41]. Subsequently, the ground state geometries of each isomer were optimized in the gas phase using the functional hybrid Becke three-parameter [42] Lee–Yang–Parr exchange–correlation functional [43, 44] (B3LYP) and the 6- 311++G(d,p) basis set with the Gaussian09 program [45]. The B3LYP functional density functional theory method with the basis set 6-311++G(d,p) was chosen since it has previously demonstrated accuracy and dependability in investigations involving aniline and aniline derivatives [46-50]. The HOMO and LUMO energy levels, chemical reactivity descriptors, non-linear optical properties, molecular electrostatic potentials map (MEP-map), natural bond orbital analysis (NBO), thermodynamic properties, and UV-Vis spectra were calculated using the same level of theory. The GaussView 5.0 program was used to visualize the results, while the GaussSum program [51] was utilized to plot the UV-Vis spectra. The adiabatic and vertical ionization parameters were calculated by optimizing the most stable molecular conformational geometry and using the same molecular geometry as the neutrals, respectively.

## **III. RESULTS AND DISCUSSION**

Conformational analysis constitutes a pivotal stage in determining the most energetically favorable configuration of a molecule. In this study, the Spartan 08 package program utilizing MMFF within molecular mechanic methods was employed for conducting conformational analysis [41]. The findings delineated singular conformer structures for each of the o-fluoroaniline, m-fluoroaniline, and p-fluoroaniline isomers (Figure 1), underscoring the robust stability of each isomer. The geometric configurations of these isomers are depicted in Figure 1, while the conformer energies and optimized energies are detailed in Table 3. Furthermore, the selected geometric parameters of the o-fluoroaniline, m-fluoroaniline, and p-fluoroaniline isomers are presented in Table 4.

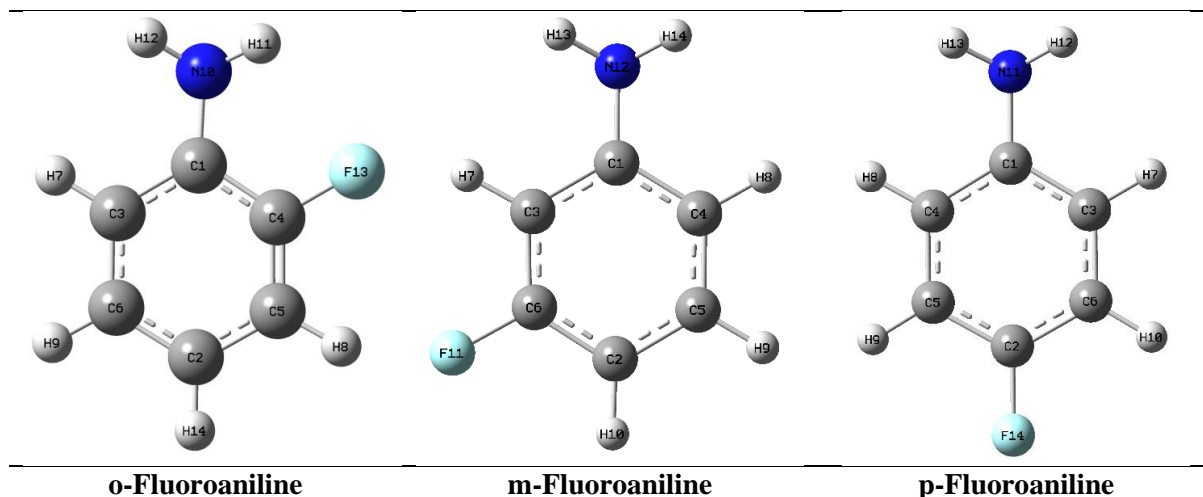


**Figure 1.** Possible conformers and the most stable structures of *o*-fluoroaniline, *m*-fluoroaniline, and *p*-fluoroaniline isomers

**Table 3.** The conformer energies and energies of optimized structures of *o*-fluoroaniline, *m*-fluoroaniline, and *p*-fluoroaniline isomers

Fluoroaniline isomers	Conformer Energies (kJ/mol)	Optimized energies (Hartree)
<i>o</i> Fluoroaniline	905.4682	-386.956300
<i>m</i> Fluoroaniline	15.9827	-386.957352
<i>p</i> Fluoroaniline	11.2923	-386.954731

**Table 4.** The selected geometric parameters of *o*-fluoroaniline, *m*-fluoroaniline, and *p*-fluoroaniline isomers

Parameters	<i>o</i> -Fluoroaniline	<i>m</i> -Fluoroaniline	<i>p</i> -Fluoroaniline	Ref [52]
<b>Bond lengths (Å)</b>				
C1-C3	1.4019	1.4028	1.4024	
C1-C4	1.3987	1.4046	1.4024	
C1-N10	1.391	-	-	
C1-N12	-	1.3937	-	
C1-N11	-	-	1.4009	
C2-C5	1.3957	1.3951	1.3849	
C2-C6	1.3938	1.3855	1.3849	
C2-H14	1.0828	-	-	1.08
C2-H10	-	1.0817	-	
C3-H7	-	-	1.085	0.94
C2-F14	-	-	1.3616	
C6-F11	-	1.3586	-	
C4-F13	1.3662	-	-	
N10-H11	1.0092	-	-	0.86
N12-H13	-	1.0089	-	
N11-H13	-	-	1.0096	
N10-F13	2.72	-	-	2.68
H11-F13	2.45	-	-	2.36
C2-F13	3.64	-	-	3.22
H14-F13	4.52	-	-	2.52
C4-H8	-	-	1.08	0.98
C4-H8	-	-	3.634	3.570
C4-F14	-	-	4.50	2.70

C3-F14	-	-	3.634	3.605
H7-F14	-	-	4.50	2.73
C5-H9	-	-	1.08	0.93
C5-N11	-	-	3.711	3.559
H9-N11	-	-	4.59	2.68
<b>Bond angle (°)</b>				
C1-N10-H11	115.5877	-	-	
C1-N12-H13	-	116.2156	-	
C1-N11-H13	-	-	115.326	
C1-N10-H12	115.8906	-	-	
C1-N12-H14	-	115.9535	-	
C1-N11-H12	-	-	115.3263	
C1-N10-C4	120.4733	-	-	
C1-N12-C3	-	120.3119	-	
C1-N11-C4	-	-	120.7199	
C1-C4-F13	117.1358	-	-	
C1-C3-H7	-	121.5045	-	
C1-C4-H8	-	-	119.6762	
C4-C5-F13	119.5111	-	-	
C3-C6-H7	-	119.5753	-	
C4-C5-H8	119.0692	-	119.4145	
C3-C6-F11	-	117.8707	-	
C4-C5-H9	-	-	121.1185	
C2-C5-H8	121.9277	-	-	
C2-C6-F11	-	118.787	-	
C2-C5-H9	-	-	119.8334	
C2-C5-H14	120.0012	-	-	
C2-C6-H10	-	120.4146	-	
C2-C5-F14	-	-	119.2012	
C2-C6-H14	120.7225	-	-	
C2-C5-H10	-	122.452	-	
C2-C6-F14	-	-	119.2019	
N10-H11-F13	100	-	-	96
C2-H14-F13	139	-	-	126
C4-H8-F14	-	-	138	150
C3-H7-F14	-	-	138	156
C5-H9-N11	-	-	140	157
<b>Dihedral angle (°)</b>				
H11-N10-C1-C3	162.7948	-	-	
H13-N12-C1-C4	-	-158.8276	-	
H13-N11-C1-C3	-	-	-157.8406	
H11-N10-C1-C4	-20.162	-	-	
H13-N12-C1-C3	-	24.0235	-	
H13-N11-C1-C4	-	-	25.2674	
H12-N10-C1-C3	26.7605	-	-	
H14-N12-C1-C4	-	-23.0641	-	
H12-N11-C1-C3	-	-	-25.2758	
H12-N10-C1-C4	-156.1963	-	-	
H14-N12-C1-C3	-	159.787	-	
H12-N11-C1-C4	-	-	157.8322	
F13-C4-C1-N10	3.36	-	-	
F11-C6-C3-H7	-	-0.4627	-	
F14-C2-C5-H9	-	-	-0.0537	
F13-C4-C5-H8	-0.3328	-	-	
F11-C6-C3-C1	-	179.8568	-	

F14-C2-C6-H10	-	-	0.0537
F13-C4-C5-C2	179.4556	-	-
F11-C6-C2-C5	-	-179.9597	-
F14-C2-C6-C3	-	-	-179.9217

In this study, we contrasted the low-temperature crystal structures of *p*-fluoroaniline and *o*-fluoroaniline, as reported by Chopra, D. et al., outcomes derived from our research, detailed in Table 4. The obtained results showed a general agreement between the experimental and theoretical datasets. Nevertheless, the crystallographic scrutiny of *m*-fluoroaniline remains outstanding, owing to the absence of pertinent experimental data in the extant literature, to our best understanding.

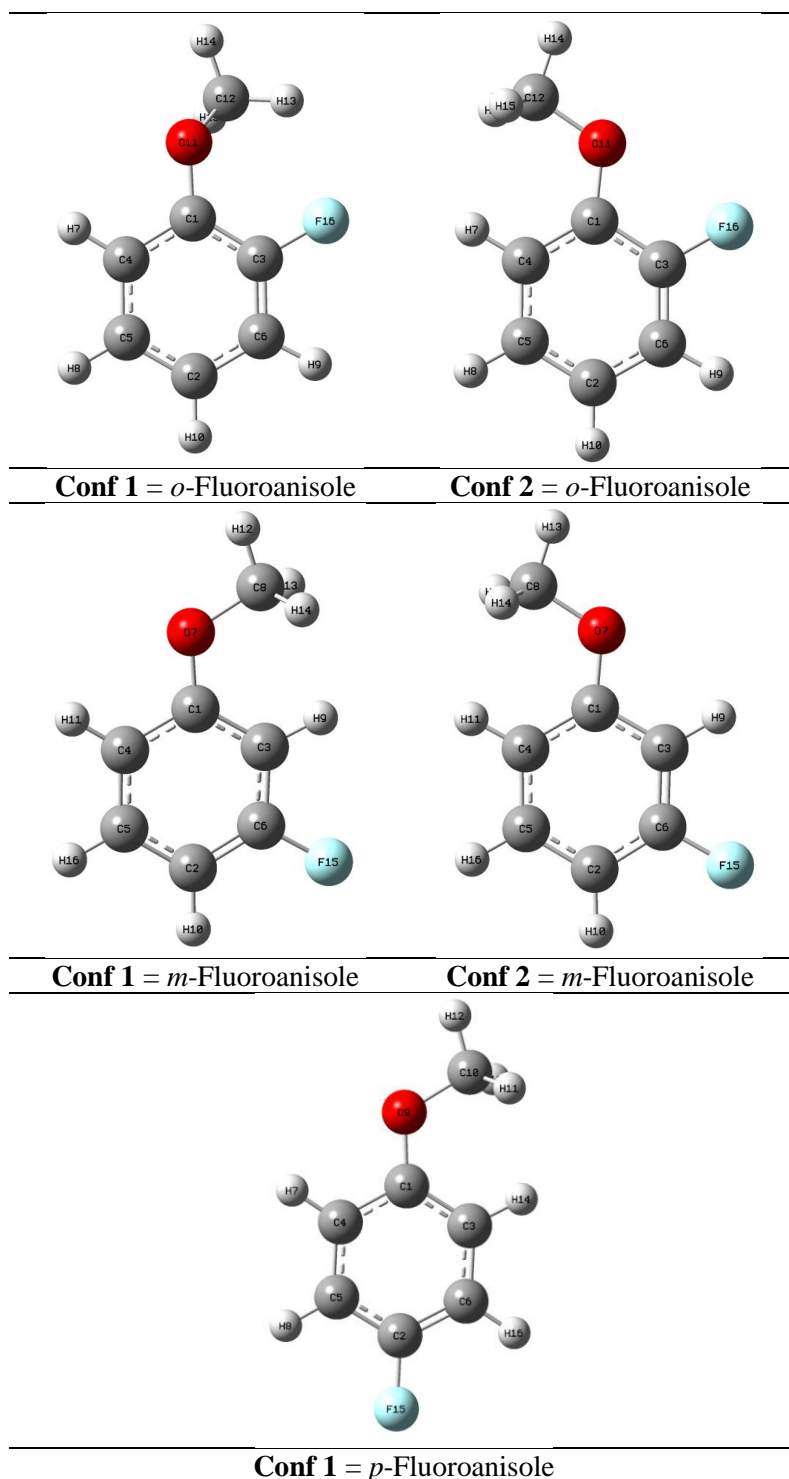




**Figure 2.** Possible conformers and the most stable structures of *o*-fluoroanisole, *m*-fluoroanisole, and *p*-fluoroanisole isomers

**Table 5.** Conformer energies and energies of optimized structures of *o*-fluoroanisole, *m*-fluoroanisole, and *p*-fluoroanisole isomers

Fluoroanisole isomers	Conformer Energies (kJ/mol)	Optimization energies (Hartree)
<b>Conf 1 = <i>o</i>-Fluoroanisole</b>	129.5518	-446.129075
<b>Conf 2 = <i>o</i>-Fluoroanisole</b>	<b>139.9477</b>	<b>-446.131300</b>
<b>Conf 1 = <i>m</i>-Fluoroanisole</b>	<b>60.0276</b>	<b>-446.136811</b>
<b>Conf 2 = <i>m</i>-Fluoroanisole</b>	60.9810	-446.136612
<b>Conf 1 = <i>p</i>-Fluoroanisole</b>	<b>70.2210</b>	<b>-446.134766</b>

A conformational analysis of each fluoroanisole isomer was conducted using the Spartan program. The results revealed the presence of two conformers, denoted as **Conf 1** and **Conf 2**, in the ortho and meta isomers (Figure 2). Conversely, only one conformer was identified in the para isomer. Table.5 presents the optimized structure and energy values of all conformers. Based on the minimum energy values for each isomer, the most stable structures were determined to be **Conf 2** for the ortho isomer, **Conf 1** for the meta isomer, and **Conf 1** for the para isomer.

**Table 6.** The selected geometric parameters of *o*-fluoroanisole, *m*-fluoroanisole, and *p*-fluoroanisole isomers

Parameters	<i>o</i> -Fluoroanisole	<i>m</i> -Fluoroanisole	<i>p</i> -Fluoroanisole
<b>Bond lengths (Å)</b>			
C1-C3	1.4030	1.3978	1.3971
C1-C4	1.3968	1.4018	1.4007
C1-O11	1.3578	-	-
C1-O7	-	1.3613	-
C12-O11	1.4220	-	-
C8-O7	-	1.4223	-
C10-O9	-	-	1.4205
C12-H14	1.0882	-	-
C8-H12	-	1.0884	-
C10-H13	-	-	1.0957
C3-F16	1.3510	-	-
C6-F15	-	1.3576	-
C2-F15	-	-	1.3593
C2-C6	1.3971	1.3816	-
C2-C5	-	-	1.3888
C3-C6	1.3800	1.3893	-
C4-C5	-	-	1.3878
<b>Bond angle (°)</b>			
O11-C12-H13	111.3754	-	-
O11-C12-H14	105.6402	-	-
O11-C12-H15	111.3746	-	-
O7-C8-H12	-	105.7863	-
O7-C8-H13	-	111.3591	-
O7-C8-H14	-	111.3589	-
O9-C10-H11	-	-	111.4521
O9-C10-H12	-	-	105.8163
O9-C10-H13	-	-	111.4512
O11-C1-C4	125.6922	-	-
C12-O11-C1	118.2856	-	-
C8-O7-C1	-	118.7370	-
O7-C1-C3	-	123.9381	-
C10-O9-C1	-	-	118.5631

O9-C1-C4	-	-	115.7157
C1-C3-F16	118.4131	-	-
C1-C3-C6	122.1193	-	-
C3-C6-F15	-	117.5447	-
C3-C6-C2	-	123.4696	-
O9-C1-C3	-	-	124.5807
C5-C2-C6	-	-	121.7921
F16-C3-C6	119.4674	-	-
F16-C3-C1	118.4131	-	-
F15-C6-C2	-	118.9856	-
F15-C6-C3	-	117.5447	-
F15-C2-C5	-	-	118.9647
F15-C2-C6	-	-	119.2431
<b>Dihedral angle (°)</b>			
C1-O11-C12-H13	-61.3113	-	-
C1-O11-C12-H14	179.9780	-	-
C1-O11-C12-H15	61.2677	-	-
C1-O7-C8-H12	-	-180	-
C1-O7-C8-H13	-	61.2963	-
C1-O7-C8-H14	-	-61.2968	-
C1-O9-C10-H11	-	-	-61.2634
C1-O9-C10-H12	-	-	-179.9851
C1-O9-C10-H13	-	-	61.2933
C12-O11-C1-C3	-179.9754	-	-
C12-O11-C1-C4	0.0283	-	-
C8-O7-C1-C3	-	-	-
C8-O7-C1-C4	-	-	-
O11-C1-C3-F16	0.0069	-	-
O7-C1-C3-C6	-	-180	-
O9-C1-C4-C5	-	-	-179.9986
F16-C3-C6-H9	-0.0040	-	-
F16-C3-C6-C2	179.9954	-	-
F15-C6-C3-H9	-	-0.0005	-
F15-C6-C3-C1	-	-179.9995	-
F15-C2-C5-H8	-	-	0.0041
F15-C2-C5-C4	-	-	-179.9969

### 3.1. Frontier Molecular Orbital (FMO) and chemical reactivity descriptors

Frontier molecular orbitals (FMOs) are critical in understanding the electronic properties and chemical reactivity of molecules. The HOMO governs the molecule's tendency to lose electrons, while the LUMO indicates the molecule's inclination to gain electrons. The isosurfaces of the molecule, where red and green colours depict positive and negative phases, offer a visual representation of the electronic distribution. The energy gap between the HOMO and LUMO dictates the stability of the chemical framework. Smaller energy gaps result in heightened chemical reactivity, elevated polarizability, and increased softness, which is a unique characteristic of the molecule. Conversely, hardness, the inverse of the softness, defines the rigidity of the molecule.

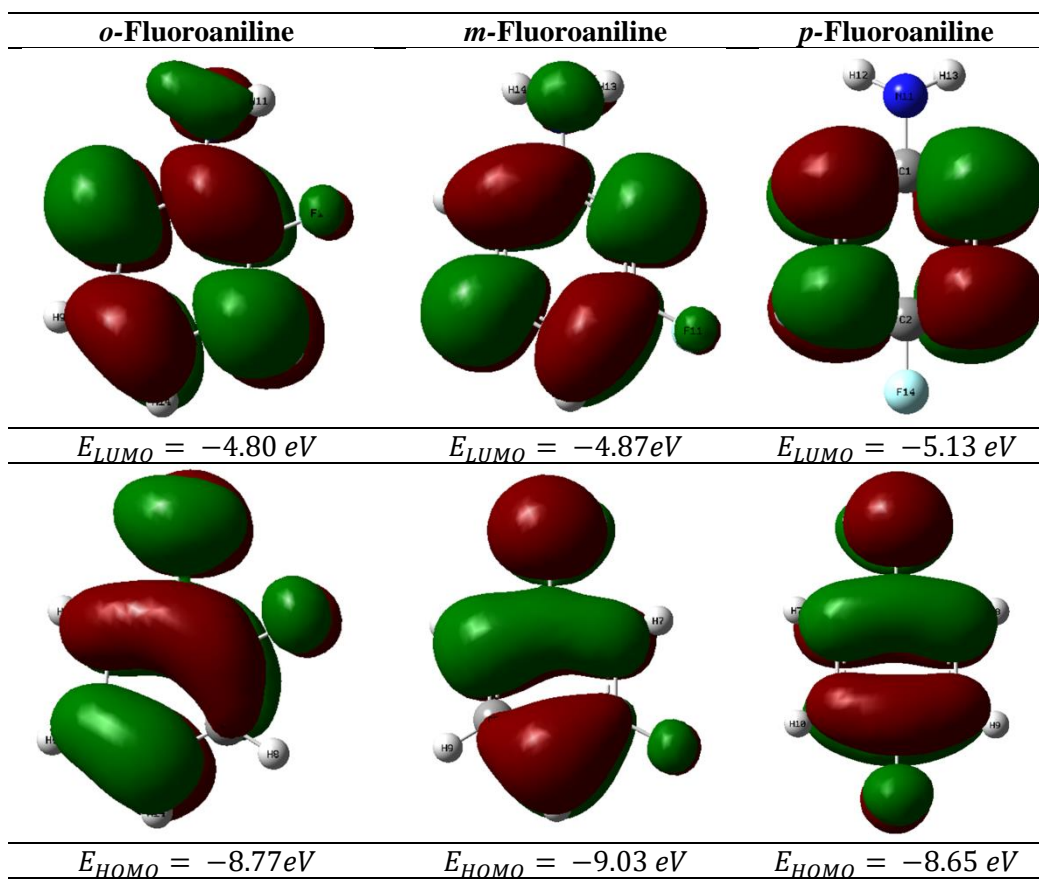


Figure 3. HOMO and LUMO for the *o*-fluoroaniline, *m*-fluoroaniline, and *p*-fluoroaniline isomers

Chemical reactivity descriptors were computed using Koopman's theorem [53]. The electron affinity (EA), ionization potential (IP), chemical potential ( $\mu$ ), chemical hardness ( $\eta$ ), softness ( $s$ ), electronegativity ( $\chi$ ), and electrophilicity index ( $\omega$ ) were calculated by utilizing the HOMO and LUMO energy values [54, 55]. The resulting values are presented in Table 7.

$$IP = -E_{HOMO} \quad (1)$$

$$EA = -E_{LUMO} \quad (2)$$

$$\mu = \frac{1}{2}[E_{LUMO} + E_{HOMO}] \quad (3)$$

$$\eta = \frac{1}{2}[E_{LUMO} - E_{HOMO}] \quad (4)$$

$$S = \frac{1}{2\eta} \quad (5)$$

$$\omega = \frac{\mu^2}{2\eta} \quad (6)$$

$$\chi = -\frac{1}{2}[E_{HOMO} + E_{LUMO}] \quad (7)$$

**Table 7.** Chemical reactivity descriptors of *o*-fluoroaniline, *m*-fluoroaniline, and *p*-fluoroaniline isomers

Isomers	$E_{gap}$ (eV)	IP (eV)	EA (eV)	$\mu$ (eV)	$\eta$ (eV)	S (eV)	$\omega$ (eV)	$\chi$ (eV)
<i>o</i> Fluoroaniline	3.97	8.77	4.80	-6.78	1.98	0.25	11.60	6.78
<i>m</i> Fluoroaniline	4.16	9.03	4.87	-6.95	2.08	0.24	11.61	6.95
<i>p</i> Fluoroaniline	3.52	8.65	5.13	-6.89	1.76	0.28	13.48	6.89

The results of the study indicate that the chemical reactivity values for the fluoroaniline isomers follow the order of *p*-fluoroaniline > *o*-fluoroaniline > *m*-fluoroaniline. Similarly, the softness values were found to be in the order of *m*-fluoroaniline > *o*-fluoroaniline > *p*-fluoroaniline, which indicates that the *m*-isomer is the most polarizable. The hardness values were found to be in the order of *p*-fluoroaniline > *o*-fluoroaniline > *m*-fluoroaniline, indicating that the *p*-isomer is the hardest. The ionization potentials of the isomers follow the order of *o*-fluoroaniline (8.77 eV) < *p*-fluoroaniline (8.65 eV) < *m*-fluoroaniline (9.03 eV), while the electron affinities are in the order of *p*-fluoroaniline (5.13 eV) > *m*-fluoroaniline (4.87 eV) > *o*-fluoroaniline (4.80 eV). Furthermore, the electrophilicity values of the isomers follow the order of *p*-fluoroaniline > *p*-fluoroaniline  $\approx$  *m*-fluoroaniline, while the electronegativity values are ranked as *m*-fluoroaniline > *p*-fluoroaniline > *o*-fluoroaniline. These findings provide valuable insights into the chemical reactivity and electronic properties of the fluoroaniline isomers.

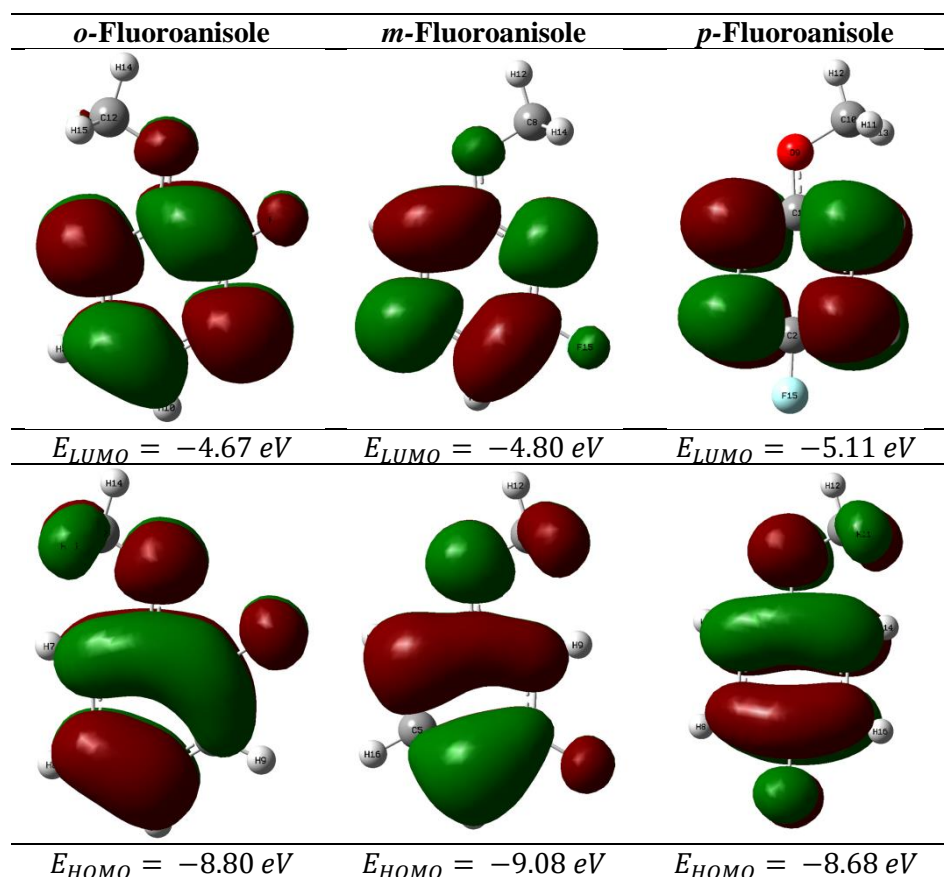


**Figure 4.** HOMO and LUMO for *o*-fluoroanisole, *m*-fluoroanisole, and *p*-fluoroanisole isomers

The highest occupied molecular orbital (HOMO) and lowest unoccupied molecular orbital (LUMO) of each fluoroanisole isomer are presented in Figure 4. The HOMO-LUMO analysis of the *o*- and *m*-fluoroanisole isomers revealed that the fluorine atoms have positive phases, while in the *p*-fluoroanisole isomer, the phases are negative. The *o*-fluoroanisole isomer has a HOMO energy of -8.80 eV and a

LUMO energy of -4.67 eV. The corresponding HOMO-LUMO gap energy for this isomer is 4.13 eV. The *m*-fluoroanisole isomer has the highest HOMO-LUMO gap energy of 4.28 eV, with a HOMO energy of -9.08 eV and a LUMO energy of -4.80 eV. On the other hand, the *p*-fluoroanisole isomer has the lowest HOMO-LUMO gap energy of 3.57 eV, with a HOMO energy of -8.68 eV and a LUMO energy of -5.11 eV. The detailed results are provided in Table 8.

**Table 8.** Chemical reactivity descriptors of *o*-fluoroanisole, *m*-fluoroanisole, and *p*-fluoroanisole isomers

Isomers	$E_{\text{gap}}$ (eV)	IP (eV)	EA (eV)	$\mu$ (eV)	$\eta$ (eV)	S (eV)	$\omega$ (eV)	$\chi$ (eV)
<i>o</i> -Fluoroanisole	4.13	8.80	4.67	-6.73	2.06	0.24	10.99	6.73
<i>m</i> -Fluoroanisole	4.28	9.08	4.80	-6.91	2.14	0.23	11.15	6.91
<i>p</i> -Fluoroanisole	3.57	8.68	5.11	-6.89	1.78	0.28	13.33	6.89

The results of the study reveal the order of chemical reactivity values for fluoroanisole isomers to be in the sequence of *m*-fluoroanisole > *o*-fluoroanisole > *p*-fluoroanisole. Additionally, the softness values for fluoroanisole isomers have been determined to be in the sequence of *p*-fluoroanisole > *o*-fluoroanisole > *m*-fluoroanisole. Based on these values, the hardness of the isomers can be ordered as *m*-fluoroanisole > *o*-fluoroanisole > *p*-fluoroanisole.

### 3.2. Non-linear optical (NLO) properties

Nonlinear optical (NLO) properties play a crucial role in the design of advanced technologies, including signal processing, optical devices, and communication systems [56]. Theoretical investigations of the NLO properties of molecules are vital in advancing such technologies. To probe the nonlinear optical behaviour, we calculated the dipole moment, polarizability, and first hyperpolarizability using the B3LYP functional with the 6-311++G(d,p) basis set. The values of dipole moment ( $\mu$ ), polarizability ( $\alpha$ ), and first-order hyperpolarizability ( $\beta$ ) were determined through the relevant equations and are presented in Table 9.

Total dipole moment ( $\mu_{tot}$ ) for a molecule is defined as in Equation 8

$$\mu_{tot} = (\mu_x + \mu_y + \mu_z)^{\frac{1}{2}} \quad (8)$$

Total polarizability ( $\alpha_{tot}$ ) for a molecule can be evaluated by Equation 9

$$\alpha_{tot} = \frac{1}{3} (\alpha_{xx} + \alpha_{yy} + \alpha_{zz}) \quad (9)$$

The total first-order hyperpolarizability ( $\beta_{tot}$ ) can be calculated by Equation 10

$$\beta_{tot} = (\beta_x^2 + \beta_y^2 + \beta_z^2)^{\frac{1}{2}} \quad (10)$$

where  $\beta_x$ ,  $\beta_y$  and  $\beta_z$  are defined to be

$$\beta_x = (\beta_{xxx} + \beta_{xyy} + \beta_{xzz}) \quad (11)$$

$$\beta_y = (\beta_{yyy} + \beta_{yzz} + \beta_{yxx}) \quad (12)$$

$$\beta_z = (\beta_{zzz} + \beta_{zxx} + \beta_{zyy}) \quad (13)$$

Total first-order hyperpolarizability from Gaussian09 output is given in Equation 14.

$$\beta_{tot} = \left[ (\beta_{xxx} + \beta_{xyy} + \beta_{xzz})^2 + (\beta_{yyy} + \beta_{yzz} + \beta_{yxx})^2 + (\beta_{zzz} + \beta_{zxx} + \beta_{zyy})^2 \right]^{\frac{1}{2}} \quad (14)$$

**Table 9.** The values of calculated dipole moment ( $\mu$ ), polarizability ( $\alpha$ ), and first-order hyperpolarizability ( $\beta$ ) components of *o*-fluoroaniline, *m*-fluoroaniline, and *p*-fluoroaniline isomers

Parameters	<i>o</i> -Fluoroaniline	<i>m</i> -Fluoroaniline	<i>p</i> -Fluoroaniline
<b>Dipole moment (Debye)</b>			
$\mu_x$	-0.1114	-2.7342	-2.9829
$\mu_y$	1.4985	0.3232	-0.0001
$\mu_z$	0.9204	0.9195	0.9878
$\mu_{tot}$	1.7621	2.9028	3.1422
<b>Polarizability (a.u)</b>			
$\alpha_{xx}$	99.574	99.823	101.922
$\alpha_{yy}$	87.529	87.972	84.278
$\alpha_{zz}$	46.926	46.769	46.478
$\alpha_{tot}$ (a.u)	78.010	78.188	77.559
$\alpha_{tot}$ (esu)	$11.561 \times 10^{-24}$	$11.587 \times 10^{-24}$	$11.494 \times 10^{-24}$
<b>Hyperpolarizability (a.u)</b>			
$\beta_{xxx}$	327.725	118.188	83.332
$\beta_{xxy}$	-64.699	215.700	0.0007
$\beta_{xyy}$	-77.891	8.781	-15.603
$\beta_{yyy}$	37.772	3.101	0.0003
$\beta_{xxz}$	10.851	10.994	8.642
$\beta_{xyz}$	1.799	1.557	0.0013
$\beta_{yyz}$	5.528	6.497	7.327
$\beta_{xzz}$	-52.144	-17.855	-34.654
$\beta_{yzz}$	17.846	36.774	-0.0006
$\beta_{zzz}$	12.612	14.336	13.853
$\beta_{tot}$ (a.u)	458.751	279.711	44.534
$\beta_{tot}$ (esu)	$3963.28 \times 10^{-33}$	$2416.50 \times 10^{-33}$	$384.74 \times 10^{-33}$

In Table.9, the total dipole moment, polarizabilities, and first-order hyperpolarizabilities of the fluoroaniline molecule isomers have been listed. Values in atomic units (a.u) obtained were converted to Statcoulomb (esu) units following using the conversion factors: for  $\mu$ , 1 a.u. = 2.5412 Debye; for  $\alpha$ , 1 a.u. =  $0.1482 \times 10^{-24}$  esu; and for  $\beta$ , 1a.u. =  $8.6393 \times 10^{-33}$  esu [23, 57-59]. The dipole moment values of all isomers were calculated in the order *p*-fluoroaniline > *m*-fluoroaniline > *o*-fluoroaniline. The polarisability of all isomers was obtained in the order *m*-fluoroaniline > *o*-fluoroaniline > *p*-fluoroaniline. The results obtained indicate that all isomers do have not a strong response to the external electric field. In addition, results show minor changes in the polarizability values among the isomers. The first-order hyperpolarizability values of all isomers were calculated in the order *o*-fluoroaniline > *m*-fluoroaniline > *p*-fluoroaniline. *o*-fluoroaniline has the highest hyperpolarizability value ( $3963.28 \times 10^{-33}$  esu). This may be because the fluorine atom is closer to the -NH<sub>2</sub>.

**Table 10.** The values of calculated dipole moment ( $\mu$ ), polarizability ( $\alpha$ ), first-order hyperpolarizability ( $\beta$ ) components of *o*-fluoroanisole, *m*-fluoroanisole, and *p*-fluoroanisole isomers

Parameters	<i>o</i> -Fluoroanisole	<i>m</i> -Fluoroanisole	<i>p</i> -Fluoroanisole
<b>Dipole moment (Debye)</b>			
$\mu_x$	-0.5125	-1.5309	2.4626
$\mu_y$	-2.7022	0.0810	-0.9387
$\mu_z$	0.0006	0	0.0004
$\mu_{tot}$	2.7504	1.5330	2.6355
<b>Polarizability (a.u)</b>			
$\alpha_{xx}$	111.193	109.785	111.954
$\alpha_{yy}$	91.169	92.541	89.538
$\alpha_{zz}$	52.967	52.731	52.576

$\alpha_{tot}$ (a.u)	85.110	85.019	84.689
$\alpha_{tot}$ (esu)	$12.613 \times 10^{-24}$	$12.599 \times 10^{-24}$	$12.551 \times 10^{-24}$
<b>Hyperpolarizability (a.u)</b>			
$\beta_{xxx}$	222.784	241.683	-12.285
$\beta_{xxy}$	-89.835	61.011	-33.706
$\beta_{xyy}$	30.452	-105.156	18.102
$\beta_{yyy}$	-164.099	40.236	-20.04
$\beta_{xxz}$	0.004	0.001	0.010
$\beta_{xyz}$	-0.008	-0.0009	0.005
$\beta_{yyz}$	-0.007	-0.0008	-0.011
$\beta_{xzz}$	36.878	15.727	23.651
$\beta_{yzz}$	-93.081	-2.152	-46.208
$\beta_{zzz}$	0.038	0.001	0.029
$\beta_{tot}$ (a.u)	452.313	181.662	104.208
$\beta_{tot}$ (esu)	$3907.66 \times 10^{-33}$	$1569.43 \times 10^{-33}$	$900.28 \times 10^{-33}$

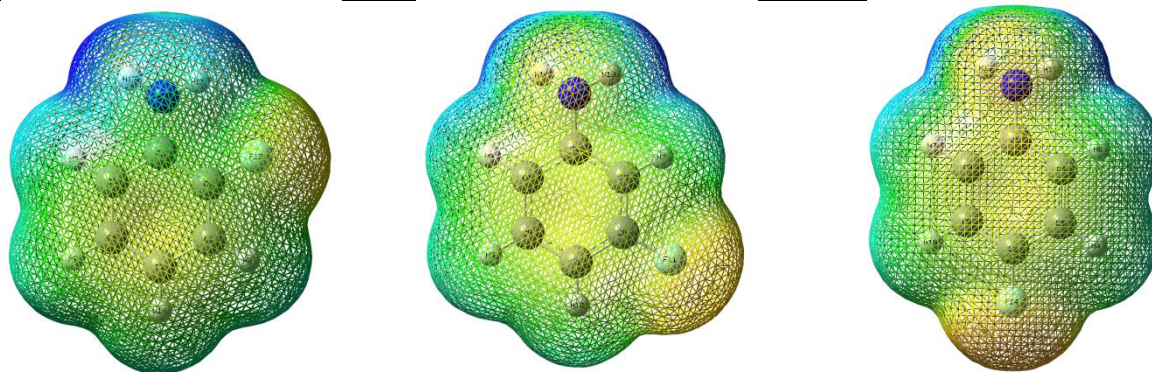
The total dipole moment, polarizabilities, and the first-order hyper-polarizabilities of the fluoroanisole molecule isomers have been listed in Table.10. The dipole moment is the most frequently used data to define the polarity of molecule systems. It is the polarity indicator of the separation of negative and positive charges between the atoms and the distance between the two bonded atoms. The dipole moment values of all isomers were calculated in the order *o*-fluoroanisole > *p*-fluoroanisole > *m*-fluoroanisole. The values of polarizability and the first-order hyper-polarizabilities are necessary to examine the NLO properties of materials. The polarizability of all isomers was obtained in the order *o*-fluoroanisole > *m*-fluoroanisole > *p*-fluoroanisole. Additionally, the first-order hyper-polarizability values of all isomers were calculated in the order *o*-fluoroanisole > *m*-fluoroanisole > *p*-fluoroanisole. *o*-fluoroanisole has the highest hyperpolarizability value ( $3907.66 \times 10^{-33}$  esu).

### 3.3. Molecular Electrostatic Potential (MEP) map

The molecular electrostatic potential (MEP) map provides a graphical representation of the electrostatic forces exerted on a unit positive charge placed at different points on a molecule. It allows for the identification of electron-rich or electron-poor regions on the surface of a molecule, which can be visualized using different colors. The MEP map is an important tool for understanding the electrophilic and nucleophilic reactivity of a molecule. Regions of the molecule with the most negative electrostatic potential are typically displayed as red, and these areas can be classified as electrophilic. Conversely, regions with the most positive electrostatic potential are generally displayed as blue, and these regions are typically nucleophilic [58, 60-62].

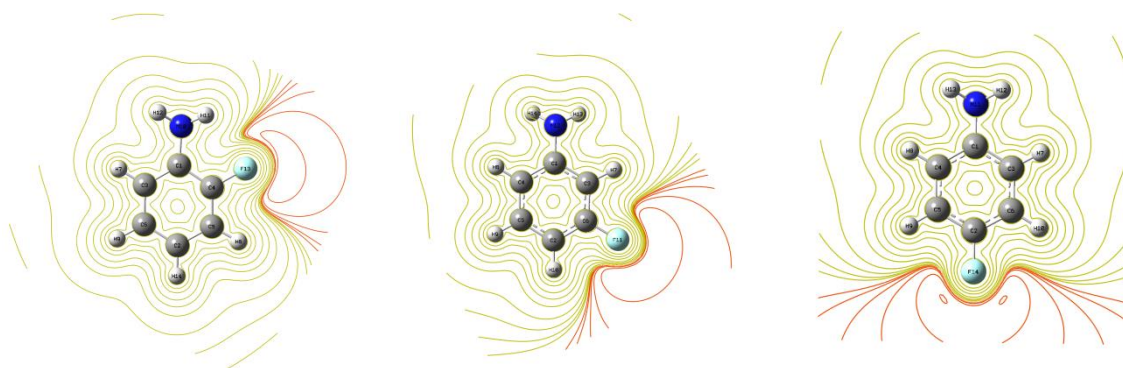
Based on the molecular electrostatic potential (MEP) map, the MEPs for all isomers exhibit comparable patterns. The negative region of each isomer is located on the fluorine atom, whereas the positive region is positioned on the amine group. The colour code of *o*-Fluoroaniline, *m*-fluoroaniline and *p*-fluoroaniline molecular range from  $-4.765 \times 10^{-2}$  a.u —  $4.765 \times 10^{-2}$  a.u,  $-4.867 \times 10^{-2}$  a.u —  $4.867 \times 10^{-2}$  a.u and  $-4.706 \times 10^{-2}$  a.u —  $4.706 \times 10^{-2}$  a.u, respectively, as illustrated in Figure 5. Furthermore, 2D contour map of electrostatic potential of the total density of fluoroaniline isomers are shown in Figure 6.





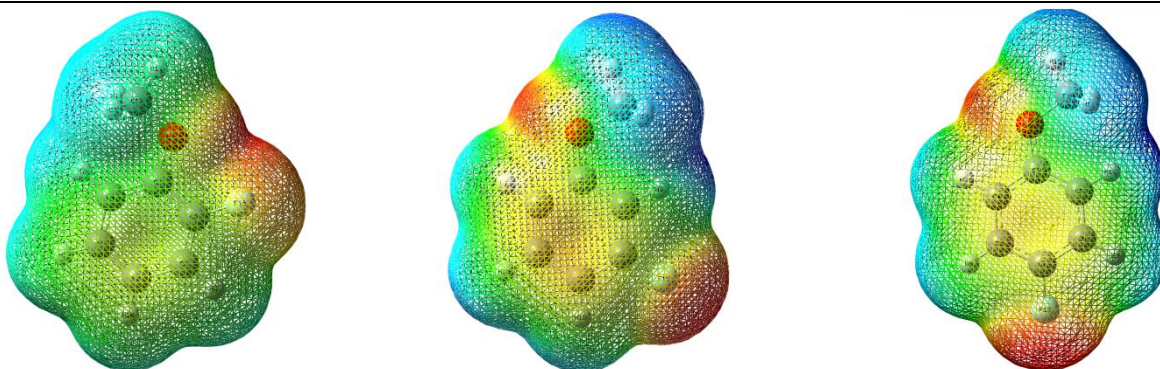
<b><i>o</i>-Fluoroaniline</b>	<b><i>m</i>-Fluoroaniline</b>	<b><i>p</i>-Fluoroaniline</b>
$-4.765 \times 10^{-2}$ a.u — $4.765 \times 10^{-2}$	$-4.867 \times 10^{-2}$ a.u — $4.867 \times 10^{-2}$	$-4.706 \times 10^{-2}$ a.u — $4.706 \times 10^{-2}$
a.u	a.u	a.u

**Figure 5.** Molecular electrostatic potential maps of *o*-fluoroaniline, *m*-fluoroaniline, and *p*-fluoroaniline isomers



<b><i>o</i>-Fluoroaniline</b>	<b><i>m</i>-Fluoroaniline</b>	<b><i>p</i>-Fluoroaniline</b>
-------------------------------	-------------------------------	-------------------------------

**Figure 6.** Contour maps of *o*-fluoroaniline, *m*-fluoroaniline, and *p*-fluoroaniline isomers



<b><i>o</i>-Fluoroanisole</b>	<b><i>m</i>-Fluoroanisole</b>	<b><i>p</i>-Fluoroanisole</b>
$-4.682 \times 10^{-2}$ a.u — $4.682 \times 10^{-2}$	$-2.823 \times 10^{-2}$ a.u — $2.823 \times 10^{-2}$	$-2.968 \times 10^{-2}$ a.u — $2.968 \times 10^{-2}$
a.u	a.u	a.u

**Figure 7.** Molecular electrostatic potential maps of *o*-fluoroanisole, *m*-fluoroanisole, and *p*-fluoroanisole isomers



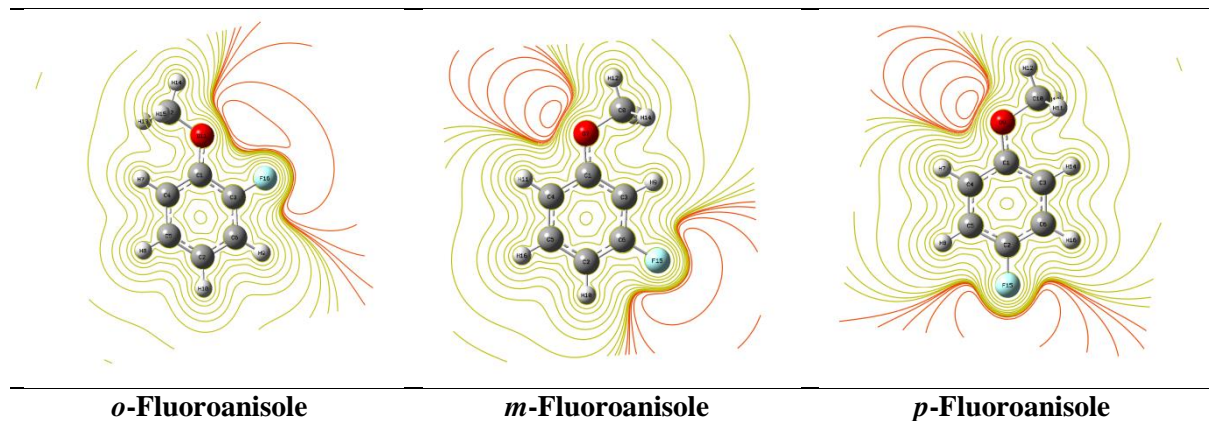


**Figure 8.** Contour maps of *o*-fluoroanisole, *m*-fluoroanisole, and *p*-fluoroanisole isomers

The molecular electrostatic potential (MEP) map provides information about the electrophilic and nucleophilic regions of molecules. The MEP maps of *o*-, *m*-, and *p*-fluoroanisole isomers are shown in Figure 7. Furthermore, 2D contour map of the electrostatic potential of the total density of fluoroanisole isomers is shown in Figure 8. The electrophilic regions, where electrophilic attacks are likely to occur, are highlighted in red, while the nucleophilic regions, where nucleophilic attacks are likely to occur, are highlighted in blue. The MEP maps demonstrate that the electrophilic regions of all isomers are primarily located on the fluorine and oxygen atoms, whereas the nucleophilic regions are primarily located on the -CH<sub>3</sub> and hydrogen atoms. The color code *o*-fluoroanisole, *m*-fluoroanisole, and *p*-fluoroanisole isomers range from  $-4.682 \times 10^{-2}$  a.u —  $4.682 \times 10^{-2}$  a.u —  $-2.823 \times 10^{-2}$  a.u —  $2.823 \times 10^{-2}$  a.u and  $-2.968 \times 10^{-2}$  a.u —  $2.968 \times 10^{-2}$  a.u respectively.

### 3.4. Natural bond orbital (NBO) analysis

The natural bond orbital analysis is a well-established and valuable technique used to study various aspects of molecular interactions, such as charge transfer and conjugative interactions. It also allows for a detailed evaluation of Lewis and non-Lewis orbitals, which contribute to intramolecular hydrogen bonding and intermolecular bonding interactions [63, 64]. This analysis provides a comprehensive description of the interaction between donor and acceptor orbitals, which is essential for understanding the underlying molecular properties. To investigate the donor and acceptor orbitals, the second-order Fock matrix was calculated for all isomers using the NBO analysis. The delocalization donor (i) → acceptor (j) stabilization energy (E<sub>2</sub>) can be determined using equation 15 [65].

$$E_2 = \Delta E_{ij} = q_i \frac{F(i,j)^2}{\epsilon_j - \epsilon_i} \quad (15)$$

Where  $q_i$  is the donor orbital occupancy,  $\epsilon_j$  and  $\epsilon_i$  are diagonal elements and  $F(i,j)^2$  is the off-diagonal NBO Fock matrix element.

Table 11 presents the nine most important values of stabilization energy (E<sub>2</sub>), orbital energies for donor and acceptor Natural Bond Orbital (NBOs), and Fock matrix for each isomer of the molecule. The NBO results, determined using second-order perturbation values of the Fock matrix, indicate that the intramolecular hydrogen bonding strength follows the order *o*-fluoroaniline > *m*-fluoroaniline > *p*-fluoroaniline.

The strongest delocalization for the *o*-fluoroaniline isomer is observed between the C4-C5 donor orbital and C2-C6 acceptor orbital, which exhibits the largest stabilizing energy. Charge transfer in this molecule is expected to occur between these bonds. The *m*-fluoroaniline isomer shows the strongest delocalization between the N12 donor orbital and C1-C3 acceptor orbital, resulting in the largest stabilizing energy. The *p*-fluoroaniline isomer, on the other hand, exhibits the strongest delocalization between the N11 donor orbital and C1-C4 acceptor orbital, again with the largest stabilizing energy.

Furthermore, if charge transfer occurs in any of these isomers, it is anticipated to occur between the bonds mentioned above.

**Table 11.** The Second order Perturbation of Fock Matrix of NBO of *o*-fluoroaniline, *m*-fluoroaniline, and *p*-fluoroaniline isomers

Isomers	Donor (i)	ED (i)	Acceptor (j)	ED (j)	E (2) (kcal/mol)	E (j) - E (i) (a.u)	F (i,j) (a.u)
<i>o</i> -Fluoroaniline	C4-C5	0.38022	C2-C6	0.36238	303.51	0.01	0.082
	N10	1.84499	C1-C3	0.4138	27.28	0.32	0.09
	C1-C3	1.64887	C2-C6	0.36238	22.32	0.29	0.072
	C2-C6	1.97902	C4-C5	0.38022	21.61	0.27	0.069
	C4-C5	1.70878	C1-C3	0.41383	20.08	0.29	0.071
	C1-C3	1.64887	C4-C5	0.38022	19.23	0.28	0.066
	C2-C6	1.97902	C1-C3	0.41383	18.3	0.27	0.065
	C4-C5	1.70878	C2-C6	0.36238	16.68	0.3	0.065
	F13	1.93724	C4-C5	0.38022	15.81	0.44	0.081
<i>m</i> -Fluoroaniline	N12	1.84420	C1-C3	0.41570	28.09	0.32	0.091
	C1-C3	1.65314	C2-C6	0.39855	27.26	0.28	0.079
	C2-C6	1.67417	C4-C5	0.34979	23.68	0.29	0.075
	C4-C5	1.71790	C1-C3	0.41570	23.43	0.28	0.074
	F11	1.92858	C2-C6	0.39855	18.06	0.43	0.086
	C2-C6	1.67417	C1-C3	0.41570	15.72	0.28	0.061
	C1-C3	1.65314	C4-C5	0.34979	15.19	0.29	0.059
	C4-C5	1.71790	C2-C6	0.39855	15.08	0.28	0.059
	F11	1.98950	C6	0.00835	8.03	2.18	0.118
<i>p</i> -Fluoroaniline	N11	1.86027	C1-C4	0.40348	25	0.33	0.087
	C1-C4	1.63949	C2-C5	0.39104	22.68	0.28	0.071
	C2-C5	1.67178	C3-C6	0.36507	21.42	0.29	0.071
	C3-C6	1.71636	C1-C4	0.40348	20.32	0.28	0.07
	C3-C6	1.71636	C2-C5	0.39104	19.03	0.28	0.067
	C1-C4	1.63949	C3-C6	0.36507	18.53	0.28	0.064
	C2-C5	1.67178	C1-C4	0.40348	17.79	0.29	0.065
	F14	1.93562	C2-C5	0.39104	16.57	0.43	0.082
	F14	1.93562	C2	0.00801	7.76	2.2	0.117

E (2): Stabilization energy.

E (j) – E (I): Energy difference of donor and acceptor orbitals.

F (i,j): Fock matrix of delocalization.

The NBO analysis provides a comprehensive account of the interaction between Lewis and non-Lewis orbitals, specifically the donor and acceptor orbitals. As depicted in Table 12, the nine most significant second-order perturbations of the Fock matrix for all isomers have been identified. Among the isomers, *o*-fluoroanisole, *m*-fluoroanisole, and *p*-fluoroanisole display strong intramolecular hyper-conjugative interactions, specifically between C1-C4 and C2-C5, C1-C3 and C4-C5, and O9 and C1-C3, respectively. These interactions are responsible for the stabilization energy, a critical parameter that determines the stability and intra-molecular charge transfer of all isomers [66]. Remarkably, the stabilization energy follows the order of *o*-fluoroanisole > *m*-fluoroanisole > *p*-fluoroanisole.

**Table 12.** The Second order Perturbation of Fock Matrix of NBO for *o*-fluoroanisole, *m*-fluoroanisole, and *p*-fluoroanisole isomers

Isomers	Donor (i)	ED (i)	Acceptor (j)	ED (j)	E (2) (kcal/mol)	E (j) – E (i) (a.u)	F (i,j) (a.u)
---------	-----------	--------	--------------	--------	------------------	---------------------	---------------

<b><i>o</i>-Fluoroanisole</b>	C1-C4	0.39864	C2-C5	0.39864	225.3	0.01	0.08
	O11	1.84061	C1-C4	0.39864	30.26	0.34	0.096
	C2-C5	1.69697	C3-C6	0.35983	20.42	0.27	0.068
	C1-C4	1.68180	C2-C5	1.69697	20.23	0.3	0.07
	C3-C6	1.98036	C1-C4	0.39864	19.52	0.29	0.069
	C2-C5	1.69697	C1-C4	0.39864	18.49	0.27	0.065
	C1-C4	1.68180	C3-C6	0.35983	18.28	0.29	0.066
	F16	1.92822	C3-C6	0.35983	17.86	0.43	0.085
	C3-C6	1.98036	C2-C5	1.69697	17.85	0.3	0.066
<b><i>m</i>-Fluoroanisole</b>	C1-C3	0.40039	C4-C5	0.32450	218.88	0.01	0.083
	O7	1.83948	C1-C3	0.40039	31.25	0.34	0.097
	C1-C3	1.68201	C2-C6	0.37548	24.84	0.29	0.077
	C4-C5	1.71250	C1-C3	0.40039	23.27	0.27	0.073
	C2-C6	1.68820	C4-C5	0.32450	22.09	0.3	0.073
	F15	1.92847	C2-C6	0.37548	18.18	0.43	0.086
	C4-C5	1.71250	C2-C6	0.37548	16.16	0.28	0.061
	C2-C6	1.68820	C1-C3	0.40039	15.72	0.28	0.061
	C1-C3	1.68201	C4-C5	0.32450	15.1	0.3	0.06
<b><i>p</i>-Fluoroanisole</b>	O9	1.84805	C1-C3	0.39064	29.32	0.34	0.095
	C1-C3	1.67187	C2-C6	0.37018	20.7	0.29	0.07
	C4-C5	1.71457	C1-C3	0.39064	20.05	0.28	0.069
	C4-C5	1.71457	C2-C6	0.37018	19.99	0.28	0.068
	C2-C6	1.68750	C4-C5	0.33372	19.96	0.3	0.069
	C1-C3	1.67187	C4-C5	0.33372	18.11	0.29	0.065
	C2-C6	1.68750	C1-C3	0.39064	17.59	0.29	0.065
	F15	1.93371	C2-C6	0.37018	17.19	0.43	0.083
	F15	1.98984	C2	0.00800	7.86	2.2	0.117

E (2): Stabilization energy.

E (j) - E(I): Energy difference of donor and acceptor orbitals.

F (i,j): Fock matrix of delocalization.

### 3.5. Thermodynamic Properties

The examination of chemical reactions necessitates an in-depth analysis of the thermodynamic parameters [67]. Table.13. presents the thermodynamic parameters of each isomer, which are of utmost importance in the scientific community. These theoretical outcomes are considered a valuable source of preliminary data for experimental work on fluoroaniline isomers. Moreover, they are instrumental in studying the intermolecular interactions between fluoroaniline isomers and other molecules.

The thermodynamic analysis of fluoroaniline isomers has yielded insightful results. It has been observed that the total energy of the *o*-fluoroaniline isomer is greater than that of the *m*-fluoroaniline isomer, which in turn is greater than that of the *p*-fluoroaniline isomer. The heat capacity of the *p*-fluoroaniline isomer is greater than that of the *m*-fluoroaniline isomer, which in turn is greater than that of the *o*-fluoroaniline isomer. Similarly, the entropy values of the isomers follow the same order. The zero-point vibrational energy, sum of electronic and zero-point energies, sum of electronic and thermal free energies, and rotational constants of the isomers have also been tabulated in Table.13.

**Table 13.** The thermodynamic parameters for *o*-fluoroaniline, *m*-fluoroaniline, and *p*-fluoroaniline isomers

Parameters	<i>o</i> - Fluoroaniline	<i>m</i> - Fluoroaniline	<i>p</i> - Fluoroaniline
Total energy (thermal), E <sub>total</sub> (kcal.mol <sup>-1</sup> )			
TOTAL	72.258	72.149	72.128
Electronic	0.000	0.000	0.000
Translational	0.889	0.889	0.889

Rotational	0.889	0.889	0.889
Vibrational	70.481	70.372	70.351
<hr/>			
Heat capacity at const. volume, $C_v$ (cal.mol <sup>-1</sup> .K <sup>-1</sup> )			
TOTAL	26.266	26.398	26.411
Electronic	0.000	0.000	0.000
Translational	2.981	2.981	2.981
Rotational	2.981	2.981	2.981
Vibrational	20.304	20.436	20.449
<hr/>			
Entropy, S (cal.mol <sup>-1</sup> .K <sup>-1</sup> )			
TOTAL	79.892	80.128	80.425
Electronic	0.000	0.000	0.000
Translational	40.030	40.030	40.030
Rotational	27.894	28.083	27.937
Vibrational	11.967	12.014	12.458
<hr/>			
Zero-point vibrational energy, $E_0$ (kcal.mol <sup>-1</sup> )			
Sum of electronic and zero-point energies (Hartree/Particle)	-386.847758	-386.849010	-386.846486
Sum of electronic and thermal free energies (Hartree/Particle)	-386.878164	-386.879501	386.877056
<hr/>			
Rotational constants (GHz)			
A	3.30655	3.72296	5.61105
B	2.21364	1.78657	1.44345
C	1.32729	1.20832	1.14923

The relative reactivity and stability of isomers can be elucidated by their thermodynamic properties. A calculated thermodynamic values table (Table 6) was used to determine the thermodynamic characteristics of fluoroanisole isomers. The results revealed that the total energy of o-fluoroanisole was greater than m-fluoroanisole and p-fluoroanisole. Heat capacity was highest in p-fluoroanisole, followed by m-fluoroanisole and then o-fluoroanisole. Entropy values followed a similar trend, with p-fluoroanisole having the highest value and m-fluoroanisole the lowest. Additionally, Table.14. presented the zero-point vibrational energy, sum of electronic and zero-point energies, sum of electronic and thermal free energies, and rotational constants values of the isomers.

**Table 14.** The thermodynamic parameters for o-fluoroanisole, m-fluoroanisole, and p-fluoroanisole isomers

Parameters	<i>o</i> - Fluoroanisole	<i>m</i> - Fluoroanisole	<i>p</i> - Fluoroanisole
<hr/>			
Total energy (thermal), $E_{total}$ (kcal.mol <sup>-1</sup> )			
TOTAL	82.810	82.729	82.680
Electronic	0.000	0.000	0.000
Translational	0.889	0.889	0.889
Rotational	0.889	0.889	0.889
Vibrational	81.032	80.951	80.903
<hr/>			
Heat capacity at const. volume, $C_v$ (cal.mol <sup>-1</sup> .K <sup>-1</sup> )			
TOTAL	29.508	29.564	29.614
Electronic	0.000	0.000	0.000
Translational	2.981	2.981	2.981
Rotational	2.981	2.981	2.981
Vibrational	23.546	23.603	23.653

Entropy, S (cal. Mol <sup>-1</sup> K <sup>-1</sup> )			
TOTAL	86.564	86.530	86.914
Electronic	0.000	0.000	0.000
Translational	40.408	40.408	40.408
Rotational	28.829	29.009	28.815
Vibrational	17.326	17.113	17.691
<hr/>			
Zero-point vibrational energy, E <sub>0</sub> (kcal.mol <sup>-1</sup> )	77.93658	77.86811	77.78749
Sum of electronic and zero-point energies (Hartree/Particle)	-446.007100	-446.012721	-446.010804
Sum of electronic and thermal free energies (Hartree/Particle)	-446.039519	-446.045144	-446.043358
<hr/>			
Rotational constants (GHz)			
A	2.52225	2.81762	4.91197
B	1.55401	1.27305	0.96536
C	0.96751	0.88180	0.81097

### 3.6. TD-DFT Results: UV-Vis Spectra and Ionization Energies

The ultraviolet-visible (UV-Vis) spectra of fluoroaniline isomers were determined using the time-dependent density functional theory (TD-DFT) approach, employing the B3LYP/6-311++G(d,p) functional and basis set. The computed spectra are depicted in Figure 9, revealing a robust absorption band around 190 nm and a comparatively weaker absorption band around 230 nm. The significant components of the UV-Vis spectra, along with their associated transitions, are tabulated in Tables 15 to 17.

The UV-Vis spectrum of the o-fluoroaniline isomer can be attributed to several leading contributions. Specifically, the transitions HOMO-1→LUMO+1, HOMO-1→LUMO+2, HOMO→LUMO+2 account for 31%, 22%, and 12% of the spectrum, respectively, with a wavelength of 193.565 nm. Furthermore, the HOMO-1→LUMO, HOMO→LUMO+2 transitions contribute 18% and 61% to the spectrum, respectively, with a wavelength of 225.061 nm. Finally, the HOMO→LUMO transition is the most prominent, accounting for 79% of the spectrum with a wavelength of 262.428 nm.

In the case of the m-fluoroaniline isomer, the leading contributions to the UV-Vis spectrum are attributed to various transitions. Notably, the HOMO-1→LUMO+3 transition accounts for 83% of the spectrum with a wavelength of 194.744 nm and energy of 6.367 eV. Additionally, the HOMO-1→LUMO, HOMO-1→LUMO+2, HOMO-1→LUMO+3, HOMO→LUMO+2, HOMO→LUMO+3, HOMO→LUMO, and HOMO→LUMO+1 transitions contribute 29%, 27%, 14%, 63%, 11%, 25%, and 63% to the spectrum, respectively, with corresponding wavelengths and energies.

For the p-fluoroaniline isomer, the leading contributions to the UV-Vis spectrum arise from the following transitions: HOMO-2→LUMO, HOMO-1→LUMO+2, HOMO-1→LUMO, HOMO→LUMO+2, HOMO→LUMO+4, and HOMO→LUMO, with corresponding percentages and wavelengths/energies. Notably, the HOMO-1→LUMO+2 transition accounts for 66% of the spectrum with a wavelength of 188.217 nm and energy of 6.588 eV, while the HOMO→LUMO transition contributes 93% of the spectrum with a wavelength of 276.207 nm and energy of 4.489 eV.

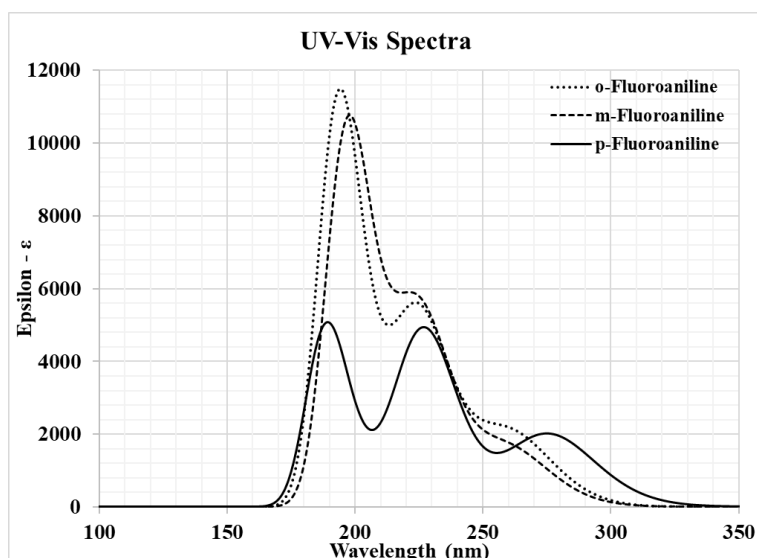


Figure 9. Calculated UV-Vis spectra of the fluoroaniline isomers (GaussSum program [51] was used to plot spectra)

Table 15. TD-DFT results for the excited states of the neutral *o*-fluoroaniline isomer (*f* is the oscillator strength)

Excited State	Energy (eV)	$\Delta E$ (nm)	<i>f</i>	Major Contributions to the Transitions (percentage)
1	4.725	262.428	0.0355	HOMO→LUMO (79%)
2	4.837	256.335	0.0151	HOMO→L+1 (86%)
3	5.238	236.710	0.0019	HOMO→L+2 (11%), HOMO→L+3 (86%)
4	5.509	225.061	0.1144	H-1→LUMO (18%), HOMO→L+2 (61%)
5	5.550	223.394	0.0145	HOMO→L+4 (87%)
6	5.969	207.713	0.0138	H-1→LUMO (14%), H-1→L+1 (75%)
7	6.076	204.069	0.0014	HOMO→L+5 (69%), HOMO→L+6 (21%)
8	6.152	201.547	0.0078	HOMO→L+5 (24%), HOMO→L+6 (71%)
9	6.247	198.492	0.0122	H-1→L+2 (10%), H-1→L+3 (83%)
10	6.406	193.565	0.2615	H-1→L (31%), H-1→L+2 (22%), H→L+2 (12%)

Table 16. TD-DFT results for the excited states of the neutral *m*-fluoroaniline isomer (*f* is the oscillator strength)

Excited State	Energy (eV)	$\Delta E$ (nm)	<i>f</i>	Major Contributions to the Transitions (percentage)
1	4.749	261.063	0.0148	HOMO→LUMO (60%), HOMO→L+1 (33%)
2	4.781	259.316	0.0241	HOMO→LUMO (25%), HOMO→L+1 (63%)
3	5.363	231.180	0.0058	HOMO→L+2 (12%), HOMO→L+3 (85%)
4	5.502	225.372	0.1177	H-1→L (11%), H→L+2 (63%), H→L+3 (11%)
5	5.619	220.675	0.0073	HOMO→L+4 (90%)
6	5.860	211.598	0.0104	H-1→LUMO (22%), H-1→L+1 (71%)
7	6.059	204.638	0.0025	HOMO→L+5 (63%), HOMO→L+6 (30%)
8	6.123	202.502	0.0133	HOMO→L+5 (31%), HOMO→L+6 (65%)
9	6.267	197.833	0.1914	H-1→L (29%), H-1→L+2 (27%), H-1→L+3 (14%)
10	6.367	194.744	0.0573	H-1→L+3 (83%)

Table 17. TD-DFT results for the excited states of the neutral *p*-fluoroaniline isomer (*f* is the oscillator strength)

Excited State	Energy (eV)	$\Delta E$ (nm)	<i>f</i>	Major Contributions to the Transitions (percentage)
1	4.489	276.207	0.0446	HOMO→LUMO (93%)
2	4.588	270.253	0.0048	HOMO→L+1 (97%)
3	5.265	235.483	0.0001	HOMO→L+3 (98%)

<b>4</b>	5.300	233.945	0.0148	HOMO→L+2 (30%), HOMO→L+4 (68%)
<b>5</b>	5.473	226.533	0.1067	H-1→L (11%), H→L+2 (56%), H→L+4 (30%)
<b>6</b>	5.906	209.925	0.0067	HOMO→L+5 (95%)
<b>7</b>	5.990	207.009	0.0	HOMO→L+6 (96%)
<b>8</b>	6.150	201.593	0.0086	H-1→L+1 (95%)
<b>9</b>	6.424	192.998	0.0207	HOMO→L+7 (89%)
<b>10</b>	6.588	188.217	0.1037	H-2→LUMO (20%), H-1→L+2 (66%)

The UV-Vis spectra of fluoroaniline isomers were computed using the TD-DFT method, with the B3LYP/6-311++G(d,p) functional and basis set. The resulting spectra are depicted in Figure 10, showing a strong absorption band at approximately 190 nm and a relatively weak absorption band at around 220 nm. The p-fluoroanisole isomer, however, exhibits a distinct absorption peak at 255 nm.

To better understand the contributions to the UV-Vis spectra, the major transitions and corresponding wavelengths and energy gaps were analyzed and are presented in Tables 18 to 20. For the o-fluoroanisole isomer, the dominant contributions originated from HOMO-1→LUMO (31%), HOMO-1→LUMO+2 (22%), and HOMO→LUMO+2 (12%) transitions, with a wavelength of 193.565 nm and an energy gap of 6.406 eV. Additionally, HOMO-1→LUMO (18%), HOMO→LUMO+2 (61%) transitions were observed at 225.061 nm with an energy gap of 5.509 eV, and HOMO-1→LUMO+3 (58%), HOMO→LUMO (79%) transitions were observed at 262.428 nm with an energy gap of 4.725 eV.

In the case of the m-fluoroanisole isomer, the leading contributions to the UV-Vis spectrum were from HOMO-1→LUMO+3 (83%) transitions, with a wavelength of 194.744 nm and an energy gap of 6.367 eV. Other significant contributions included HOMO-1→LUMO (29%), HOMO-1→LUMO+2 (27%), and HOMO-1→LUMO+3 (14%) transitions at 197.833 nm with an energy gap of 6.267 eV, as well as HOMO-1→LUMO (11%), HOMO→LUMO+2 (63%), and HOMO→LUMO+3 (11%) transitions at 225.061 nm with an energy gap of 5.509 eV. A final significant transition was HOMO→LUMO (25%), HOMO→LUMO+1 (63%) at 259.316 nm with an energy gap of 4.781 eV.

Finally, for the p-fluoroanisole isomer, the dominant contributions to the UV-Vis spectrum originated from HOMO-2→LUMO (20%), HOMO-1→LUMO+2 (66%) transitions at a wavelength of 188.217 nm with an energy gap of 6.588 eV. Other significant transitions were observed at 226.533 nm with an energy gap of 5.473 eV, including HOMO-1→LUMO (11%), HOMO→LUMO+2 (56%), and HOMO→LUMO+4 (30%) transitions, as well as HOMO→LUMO (93%) transitions at 276.207 nm with an energy gap of 4.489 eV.

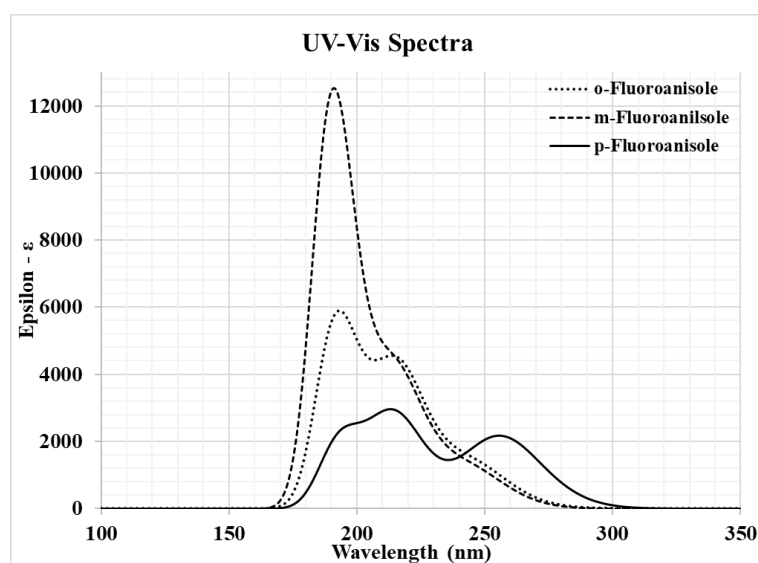


Figure 10. Calculated UV-Vis spectra of the fluoroaniline isomers (GaussSum program [51] was used to plot spectra)

**Table 18.** TD-DFT results for the excited states of the neutral *o*-fluoroanisole isomer (*f* is the oscillator strength)

Excited State	Energy (eV)	$\Delta E$ (nm)	<i>f</i>	Major Contributions to the Transitions (percentage)
1	4.725	262.428	0.0355	HOMO→LUMO (79%)
2	4.837	256.335	0.0151	HOMO→L+1 (86%)
3	5.238	236.710	0.0019	HOMO→L+2 (11%), HOMO→L+3 (86%)
4	5.509	225.061	0.1144	H-1→LUMO (18%), HOMO→L+2 (61%)
5	5.550	223.394	0.0145	HOMO→L+4 (87%)
6	5.969	207.713	0.0138	H-1→LUMO (14%), H-1→L+1 (75%)
7	6.076	204.069	0.0014	HOMO→L+5 (69%), HOMO→L+6 (21%)
8	6.152	201.547	0.0078	HOMO→L+5 (24%), HOMO→L+6 (71%)
9	6.247	198.492	0.0122	H-1→L+2 (10%), H-1→L+3 (83%)
10	6.406	193.565	0.2615	H-1→L (31%), H-1→L+2 (22%), H→L+2 (12%)

**Table 19.** TD-DFT results for the excited states of the neutral *m*-fluoroanisole isomer (*f* is the oscillator strength)

Excited State	Energy (eV)	$\Delta E$ (nm)	<i>f</i>	Major Contributions to the Transitions (percentage)
1	4.749	261.063	0.0148	HOMO→LUMO (60%), HOMO→L+1 (33%)
2	4.781	259.316	0.0241	HOMO→LUMO (25%), HOMO→L+1 (63%)
3	5.363	231.180	0.0058	HOMO→L+2 (12%), HOMO→L+3 (85%)
4	5.502	225.372	0.1177	H-1→L (11%), H→L+2 (63%), H→L+3 (11%)
5	5.619	220.675	0.0073	HOMO→L+4 (90%)
6	5.860	211.598	0.0104	H-1→LUMO (22%), H-1→L+1 (71%)
7	6.059	204.638	0.0025	HOMO→L+5 (63%), HOMO→L+6 (30%)
8	6.123	202.502	0.0133	HOMO→L+5 (31%), HOMO→L+6 (65%)
9	6.267	197.833	0.1914	H-1→L (29%), H-1→L+2 (27%), H-1→L+3 (14%)
10	6.367	194.744	0.0573	H-1→L+3 (83%)

**Table 20.** TD-DFT results for the excited states of the neutral *p*-fluoroanisole isomer (*f* is the oscillator strength)

Excited State	Energy (eV)	$\Delta E$ (nm)	<i>f</i>	Major Contributions to the Transitions (percentage)
1	4.489	276.207	0.0446	HOMO→LUMO (93%)
2	4.588	270.253	0.0048	HOMO→L+1 (97%)
3	5.265	235.483	0.0001	HOMO→L+3 (98%)
4	5.300	233.945	0.0148	HOMO→L+2 (30%), HOMO→L+4 (68%)
5	5.473	226.533	0.1067	H-1→L (11%), H→L+2 (56%), H→L+4 (30%)
6	5.906	209.925	0.0067	HOMO→L+5 (95%)
7	5.990	207.009	0.0	HOMO→L+6 (96%)
8	6.150	201.593	0.0086	H-1→L+1 (95%)
9	6.424	192.998	0.0207	HOMO→L+7 (89%)
10	6.588	188.217	0.1037	H-2→LUMO (20%), H-1→L+2 (66%)

The ionization of *o*-, *m*-, and *p*-fluoroaniline isomers was studied through adiabatic and vertical methods. The resulting minimum energies were found to be -386.672, -386.671, and -386.676 Hartree for the *o*-, *m*-, and *p*-isomers, respectively. These energies correspond to 0.284, 0.287, and 0.278 Hartree relative to their respective neutrals. The minimum energies for the vertically ionized isomers were -386.533, -386.657, and -386.662 Hartree, with respective energy reductions of 0.423, 0.301, and 0.293 Hartree compared to their neutrals. The dipole moment values for both adiabatically and vertically ionized molecules followed the order para>meta>ortho, similar to their respective neutrals.

Similarly, the ionization of *o*-, *m*-, and *p*-fluoroanisole isomers was studied, and the resulting minimum energies were -445.831, -445.834, and -445.839 Hartree, corresponding to 0.300, 0.303, and 0.296



Hartree relative to their respective neutrals. The minimum energies for the vertically ionized isomers were -445.822, -445.825, and -445.829 Hartree, with respective energy reductions of 0.309, 0.312, and 0.306 Hartree compared to their neutrals. The dipole moment values for both adiabatically and vertically ionized molecules followed the order ortho>para>meta, similar to their respective neutrals.

Koopman's theorem was employed to calculate the chemical reactivity descriptors of fluoroaniline and fluoroanisole isomers, as presented in Table 7 and Table 8. This was done by utilizing the HOMO and LUMO energy values. To further examine these findings, vertical and adiabatic ionization energy parameters were also determined by creating singly charged cation radicals. Previous studies have employed comparable techniques to investigate the isomers of xylene [68] and xylenol [69].

The ionization potentials for the isomers of o-fluoroaniline, m-fluoroaniline, and p-fluoroaniline were computed to be 8.77, 9.03, and 8.65 eV, respectively. The adiabatic and vertical ionization values were tabulated in Table 21. The adiabatic ionization energies were determined to be 7.726, 7.798, and 7.573 eV for o-, m-, and p-fluoroaniline, respectively. These findings are in close agreement with experimental data [10-12]. Furthermore, the vertical ionization energies were calculated to be 11.506, 8.187, and 7.961 eV for o-, m-, and p-fluoroaniline, respectively.

The ionization potentials of the isomeric forms of o-fluoroanisole, m-fluoroanisole, and p-fluoroanisole have been calculated and are presented in Table 8. The values obtained for o-fluoroanisole, m-fluoroanisole, and p-fluoroanisole are 8.80, 9.08, and 8.68 eV, respectively. Adiabatic ionization energies of these compounds were also determined and found to be 8.169, 8.253, and 8.058 eV for o-, m-, and p-fluoroanisole, respectively. The values obtained from these calculations are in good agreement with experimental results [28, 31]. Additionally, the vertical ionization energies were determined and found to be 8.411, 8.477, and 8.319 eV for o-, m-, and p-fluoroanisole, respectively.

**Table 21.** Molecular energies (relative to its neutrals) and dipole moments of the fluoroaniline and fluoroanisole isomers (AI: Adiabatic Ionization, VI: Vertical Ionization)

Isomers	Energy (Hartree)	Relative Energy (Hartree)	Relative Energy (kcal/mol)	Relative Energy (cm <sup>-1</sup> )	Relative Energy (eV)	Dipole Moment (D)
<b>o-fluoroaniline (AI)</b>	-386.672	0.284	178.162	62311.703	7.726	3.007
<b>m-fluoroaniline (AI)</b>	-386.671	0.287	179.821	62891.762	7.798	5.499
<b>p-fluoroaniline (AI)</b>	-386.676	0.278	174.623	61073.892	7.573	5.905
<b>o-fluoroaniline (VI)</b>	-386.533	0.423	265.319	92794.769	11.506	4.174
<b>m-fluoroaniline (VI)</b>	-386.657	0.301	188.784	66026.672	8.187	5.087
<b>p-fluoroaniline (VI)</b>	-386.662	0.293	183.572	64203.754	7.961	5.531
<b>o-fluoroanisole (AI)</b>	-445.831	0.300	188.380	65885.333	8.169	3.680
<b>m-fluoroanisole (AI)</b>	-445.834	0.303	190.321	66564.373	8.253	2.073
<b>p-fluoroanisole (AI)</b>	-445.839	0.296	185.818	64989.237	8.058	3.119
<b>o-fluoroanisole (VI)</b>	-445.822	0.309	193.953	67834.665	8.411	4.098
<b>m-fluoroanisole (VI)</b>	-445.825	0.312	195.473	68366.002	8.477	2.055

<b>p-fluoroanisole (VI)</b>	-445,829	0,306	191.832	67092.637	8.319	3.147
---------------------------------	----------	-------	---------	-----------	-------	-------

## IV. CONCLUSION

The present study investigated two significant aromatic compounds, fluoroaniline and fluoroanisole isomers, through theoretical methods. Firstly, molecular structure optimization was carried out, followed by conformational analysis to identify the most stable isomer structure. Furthermore, nonlinear optics properties (NLO), frontier molecular orbital energies (HOMO-1, HOMO/SOMO, LUMO, LUMO+1), and chemical reactivity descriptors, including ionization potentials (vertical and adiabatic), electron affinity, chemical hardness, softness, and electronegativity, were calculated using density functional theory method with B3LYP functional and 6-311++G (d, p) basis set. The molecular electrostatic potential (MEP), natural bonding orbital (NBO), and UV-Vis spectra were also obtained, along with the first ten excited states energies and oscillator strengths. Additionally, the vertical and adiabatic ionization energy parameters were investigated through the construction of the singly charged cation radicals. The results obtained through this method were found to be more reliable for calculating the ionization energies of the titled molecules compared to Koopman's theorem.

**ACKNOWLEDGEMENTS:** This work was supported by the Scientific and Technical Research Council of Turkey (TUBITAK) under Grant No. 118C476 and Grant No. 122F301. However, the entire responsibility of the publication belongs to the authors of the publication. The financial support received from TÜBİTAK does not mean that the content of the publication is approved in a scientific sense by TÜBİTAK.

## V. REFERENCES

- [1] I. M. Rietjens and J. Vervoort, "Microsomal metabolism of fluoroanilines," *Xenobiotica*, vol. 19, no. 11, pp. 1297-1305, 1989.
- [2] K. Haruna, A. A. Alenaizan, and A. A. Al-Saadi, "Density functional theory study of the substituent effect on the structure, conformation and vibrational spectra in halosubstituted anilines," *RSC Advances*, vol. 6, no. 72, pp. 67794-67804, 2016.
- [3] M. Shashidhar, K. S. Rao, and E. Jayadevappa, "Vibrational spectra of ortho-, meta and para-fluoroanilines," *Spectrochimica Acta Part A: Molecular Spectroscopy*, vol. 26, no. 12, pp. 2373-2377, 1970.
- [4] R. Kydd and P. Krueger, "The far-infrared vapor phase spectra of some halosubstituted anilines," *The Journal of Chemical Physics*, vol. 69, no. 2, pp. 827-832, 1978.
- [5] R. D. Gordon, D. Clark, J. Crawley, and R. Mitchell, "Excited state amino inversion potentials in aniline derivatives: Fluoroanilines and aminopyridines," *Spectrochimica Acta Part A: Molecular Spectroscopy*, vol. 40, no. 7, pp. 657-668, 1984.
- [6] M. Becucci, E. Castellucci, I. Lopez-Tocon, G. Pietraperzia, P. Salvi, and W. Caminati, "Inversion Motion and S1 Equilibrium Geometry of 4-Fluoroaniline: Molecular Beam High-Resolution Spectroscopy and ab Initio Calculations," *The Journal of Physical Chemistry A*, vol. 103, no. 45, pp. 8946-8951, 1999.

- [7] M. H. Palmer, W. Moyes, M. Speirs, and J. N. A. Ridyard, "The electronic structure of substituted benzenes; ab initio calculations and photoelectron spectra for phenol, the methyl- and fluoro-derivatives, and the dihydroxybenzenes," *Journal of Molecular Structure*, vol. 52, pp. 293-307, 1979.
- [8] C. H. Sin, R. Tembreull, and D. M. Lubman, "Resonant two-photon ionization spectroscopy in supersonic beams for discrimination of disubstituted benzenes in mass spectrometry," *Analytical Chemistry*, vol. 56, no. 14, pp. 2776-2781, 1984.
- [9] R. Tembreull, T. M. Dunn, and D. M. Lubman, "Excited state spectroscopy of para disubstituted benzenes in a supersonic beam using resonant two photon ionization," *Spectrochimica Acta Part A: Molecular Spectroscopy*, vol. 42, no. 8, pp. 899-906, 1986.
- [10] W. Tzeng and J. Lin, "Ionization energy of p-fluoroaniline and vibrational levels of p-fluoroaniline cation determined by mass-analyzed threshold ionization spectroscopy," *The Journal of Physical Chemistry A*, vol. 103, no. 43, pp. 8612-8619, 1999.
- [11] J. L. Lin and W. B. Tzeng, "Ionization energy of o-fluoroaniline and vibrational levels of o-fluoroaniline cation determined by mass-analyzed threshold ionization spectroscopy," *Physical Chemistry Chemical Physics*, vol. 2, no. 17, pp. 3759-3763, 2000.
- [12] J. L. Lin, K. C. Lin, and W. B. Tzeng, "Species-selected mass-analyzed threshold ionization spectra of m-fluoroaniline cation," (in English), *Applied Spectroscopy*, vol. 55, no. 2, pp. 120-124, Feb 2001.
- [13] S. P. Mirza, N. P. Raju, and M. Vairamani, "Estimation of the proton affinity values of fifteen matrix-assisted laser desorption/ionization matrices under electrospray ionization conditions using the kinetic method," *Journal of the American Society for Mass Spectrometry*, vol. 15, no. 3, pp. 431-435, 2004.
- [14] H. Borsdorf, E. Nazarov, and R. Miller, "Time-of-flight ion mobility spectrometry and differential mobility spectrometry: A comparative study of their efficiency in the analysis of halogenated compounds," *Talanta*, vol. 71, no. 4, pp. 1804-1812, 2007.
- [15] G. Chałasiński and M. M. Szcześniak, "State of the art and challenges of the ab initio theory of intermolecular interactions," *Chemical reviews*, vol. 100, no. 11, pp. 4227-4252, 2000.
- [16] A. Abdou, H. M. Mostafa, and A.-M. M. Abdel-Mawgoud, "Seven metal-based bi-dentate NO azocoumarine complexes: Synthesis, physicochemical properties, DFT calculations, drug-likeness, in vitro antimicrobial screening and molecular docking analysis," *Inorganica Chimica Acta*, vol. 539, p. 121043, 2022.
- [17] S. Bahçeli, E. K. Sarıkaya, and Ö. Dereli, "5-Bromosalicylaldehyde: Theoretical, Experimental and Spectroscopic (FT-IR, Raman, H1 and C13-NMR, UV-Vis) Studies and Their Photovoltaic Parameters," *ChemistrySelect*, vol. 9, no. 12, p. e202400054, 2024.
- [18] E.-W. Huang et al., "Machine-learning and high-throughput studies for high-entropy materials," *Materials Science and Engineering: R: Reports*, vol. 147, p. 100645, 2022.
- [19] M. A. Baldwin, A. G. Loudon, A. Maccoll, and K. S. Webb, "The nature and fragmentation pathways of the molecular ions of some arylureas, arylthioureas, acetanilides, thioacetanilides and related compounds," *Journal of Mass Spectrometry*, vol. 11, no. 11, pp. 1181-1193, 1976.

- [20] G. G. Furin, A. S. Sultanov, and I. I. Furlei, "Photoelectronic spectra of fluorine-containing aromatic amines," (in English), *Bulletin of the Academy of Sciences of the USSR Division of Chemical Science*, vol. 36, no. 3, pp. 530-534, Mar 1987.
- [21] M. H. Palmer, W. Moyes, and M. Spiers, "The electronic structure of substituted benzenes: ab initio calculations and photoelectron spectra for benzonitrile, the tolunitriles, fluorobenzonitriles, dicyanobenzenes and ethynylbenzene," (in English), *Journal of Molecular Structure*, vol. 62, no. Feb, pp. 165-187, 1980.
- [22] P. Farrell and J. Newton, "Ionization potentials of primary aromatic amines and aza-hydrocarbons," *Tetrahedron Letters*, vol. 7, no. 45, pp. 5517-5523, 1966.
- [23] I. C. de Silva, R. M. de Silva, and K. N. De Silva, "Investigations of nonlinear optical (NLO) properties of Fe, Ru and Os organometallic complexes using high accuracy density functional theory (DFT) calculations," vol. 728, no. 1-3, pp. 141-145, 2005.
- [24] H. Seip and R. Seip, "On the Structure of Gaseous Anisole," *Acta Chem. Scand*, vol. 27, pp. 4024-4027, 1973.
- [25] O. Desyatnyk, L. Pszczółkowski, S. Thorwirth, T. Krygowski, and Z. Kisiel, "The rotational spectra, electric dipole moments and molecular structures of anisole and benzaldehyde," *Physical Chemistry Chemical Physics*, vol. 7, no. 8, pp. 1708-1715, 2005.
- [26] C. Eisenhardt, G. Pietraperzia, and M. Becucci, "The high resolution spectrum of the S 1← S 0 transition of anisole," *Physical Chemistry Chemical Physics*, vol. 3, no. 8, pp. 1407-1410, 2001.
- [27] M. Bossa, S. Morpurgo, and S. Stranges, "The use of ab initio and DFT calculations in the interpretation of ultraviolet photoelectron spectra: the rotational isomerism of anisole and thioanisole as a case study," *Journal of Molecular Structure: THEOCHEM*, vol. 618, no. 1, pp. 155-164, 2002.
- [28] M. Pradhan, C. Li, J. L. Lin, and W. B. Tzeng, "Mass analyzed threshold ionization spectroscopy of anisole cation and the OCH<sub>3</sub> substitution effect," *Chemical physics letters*, vol. 407, no. 1, pp. 100-104, 2005.
- [29] I. B. Khalifa et al., "About some properties of electro-synthesized short Oligo (Para-Fluoro-Anisole)(OPFA): A combined experimental and theoretical study," *Journal of Molecular Structure*, vol. 997, no. 1, pp. 37-45, 2011.
- [30] D. Xiao et al., "Vibrational spectrum of p-fluoroanisole in the first excited state (S 1) and ab initio calculations," *Journal of Molecular Structure*, vol. 882, no. 1, pp. 56-62, 2008.
- [31] K. S. Shiung, D. Yu, H. C. Huang, and W. B. Tzeng, "Rotamers of m-fluoroanisole studied by two-color resonant two-photon mass-analyzed threshold ionization spectroscopy," *Journal of Molecular Spectroscopy*, vol. 274, pp. 43-47, 2012.
- [32] B. Bogdanov, D. van Duijn, S. Ingemann, and S. Hammerum, "Protonation of fluorophenols and fluoroanisoles in the gas phase: experiment and theory," *Physical Chemistry Chemical Physics*, vol. 4, no. 13, pp. 2904-2910, 2002.
- [33] P. Brown, "Kinetic studies in mass spectrometry—VIII: Competing [M<sup>+</sup>CH<sub>3</sub>] and [M<sup>+</sup>CH<sub>2</sub>O] reactions in substituted anisoles. Approximate activation energies from ionization and appearance potentials," *Organic Mass Spectrometry*, vol. 4, no. S1, pp. 519-532, 1970.

- [34] M. A. R. da Silva and A. I. L. Ferreira, "Experimental and computational study on the molecular energetics of the three monofluoroanisole isomers," *The Journal of Chemical Thermodynamics*, vol. 41, no. 3, pp. 361-366, 2009.
- [35] N. I. Giricheva, G. V. Girichev, J. S. Levina, and H. Oberhammer, "Molecular structures and conformations of 4-fluoroanisole and 3, 4-difluoroanisole: gas electron diffraction and quantum chemical calculations," *Journal of molecular structure*, vol. 703, no. 1, pp. 55-62, 2004.
- [36] V. P. Novikov, L. V. Vilkov, and H. Oberhammer, "Conformational properties of 2-fluoroanisole in the gas phase," *The Journal of Physical Chemistry A*, vol. 107, no. 6, pp. 908-913, 2003.
- [37] T. Isozaki, K. Sakeda, T. Suzuki, and T. Ichimura, "Fluorescence spectroscopy of jet-cooled o-fluoroanisole: Mixing through Duschinsky effect and Fermi resonance," *The Journal of chemical physics*, vol. 132, no. 21, p. 214308, 2010.
- [38] S. G. Lias and P. Ausloos, "Ionization energies of organic compounds by equilibrium measurements," *Journal of the American Chemical Society*, vol. 100, no. 19, pp. 6027-6034, 1978.
- [39] K. Watanabe, T. Nakayama, and J. Mottl, "Ionization potentials of some molecules," *Journal of Quantitative Spectroscopy and Radiative Transfer*, vol. 2, no. 4, pp. 369-382, 1962.
- [40] A. Oikawa, H. Abe, N. Mikami, and M. Ito, "Electronic spectra and ionization potentials of rotational isomers of several disubstituted benzenes," *Chemical physics letters*, vol. 116, no. 1, pp. 50-54, 1985.
- [41] Y. Shao et al., "Spartan'08, Wavefunction, Inc. Irvine, CA," vol. 8, pp. 3172-3191, 2006.
- [42] A. D. Becke, "Density-functional exchange-energy approximation with correct asymptotic behavior," *Physical Review A*, vol. 38, no. 6, pp. 3098-3100, 09/01/ 1988.
- [43] C. Lee, W. Yang, and R. G. Parr, "Development of the Colle-Salvetti correlation-energy formula into a functional of the electron density," *Physical review B*, vol. 37, no. 2, p. 785, 1988.
- [44] B. Miehlich, A. Savin, H. Stoll, and H. Preuss, "Results obtained with the correlation energy density functionals of Becke and Lee, Yang and Parr," *Chemical Physics Letters*, vol. 157, no. 3, pp. 200-206, 1989.
- [45] M. Frisch et al., "Gaussian 09, revision D. 01," ed: Gaussian, Inc., Wallingford CT, 2009.
- [46] V. Balachandran, G. Santhi, V. Karpagam, and A. Lakshmi, "DFT computation and spectroscopic analysis of N-(p-methoxybenzylidene) aniline, a potentially useful NLO material," *Journal of Molecular Structure*, vol. 1047, pp. 249-261, 2013.
- [47] E. Enbaraj et al., "Novel Synthesis of NE, N' E-4, 4'-sulfonylbis (N-(substituted-dichlorobenzylidene) anilines derivative their application biological and DFT studies," in *Journal of Physics: Conference Series*, 2021, vol. 1724, no. 1, p. 012046: IOP Publishing.
- [48] N. Kang, Z.-X. Zhao, and H.-X. Zhang, "Mechanistic Study on CpRh (III)-Catalyzed [3+ 2] Annulation of Aniline Derivatives with Vinylsilanes: A DFT Study," *The Journal of Organic Chemistry*, vol. 88, no. 11, pp. 7320-7327, 2023.

- [49] H. T. Le, R. Flammang, M. Barbieux-Flammang, P. Gerbaux, and M. T. Nguyen, "Ionized aniline and its distonic radical cation isomers," *International Journal of Mass Spectrometry*, vol. 217, no. 1-3, pp. 45-54, 2002.
- [50] A. R. Kumar et al., "Comparison of spectroscopic, structural, and molecular docking studies of 5-nitro-2-fluoroaniline and 2-nitro-5-fluoroaniline: An attempt on fluoroaniline isomers," *Journal of Fluorine Chemistry*, vol. 270, p. 110167, 2023.
- [51] N. M. O'boyle, A. L. Tenderholt, and K. M. Langner, "Cclib: a library for package-independent computational chemistry algorithms," *Journal of computational chemistry*, vol. 29, no. 5, pp. 839-845, 2008.
- [52] D. Chopra, V. Thiruvengadam, T. N. G. J. C. g. Row, and design, "In situ cryo-crystallization of fluorinated amines: A comparative study of cooperative intermolecular interactions involving ordered and disordered fluorine," vol. 6, no. 4, pp. 843-845, 2006.
- [53] T. Koopmans, "Über die Zuordnung von Wellenfunktionen und Eigenwerten zu den einzelnen Elektronen eines Atoms," vol. 1, no. 1-6, pp. 104-113, 1934.
- [54] L. Pauling, *The Nature of the Chemical Bond*. Cornell university press Ithaca, NY, 1960.
- [55] R. G. Parr, L. v. Szentpaly, and S. Liu, "Electrophilicity index," vol. 121, no. 9, pp. 1922-1924, 1999.
- [56] P. S. Liyanage, R. M. de Silva, and K. N. de Silva, "Nonlinear optical (NLO) properties of novel organometallic complexes: high accuracy density functional theory (DFT) calculations," vol. 639, no. 1-3, pp. 195-201, 2003.
- [57] P. N. Prasad and D. J. Williams, *Introduction to nonlinear optical effects in molecules and polymers*. Wiley New York, 1991.
- [58] Y. Ekincioglu, H. Ş. Kılıç, and Ö. Dereli, "DFT Study of Conformational Analysis, Molecular Structure and Properties of para-, meta-and ortho 4-Methoxyphenyl Piperazine Isomers," pp. 1-11, 2021.
- [59] A. Zawadzka et al., "Optical and structural characterization of thin films containing metallophthalocyanine chlorides," *Dyes and Pigments*, vol. 112, pp. 116-126, 2015.
- [60] I. Alkorta and J. J. Perez, "Molecular polarization potential maps of the nucleic acid bases," vol. 57, no. 1, pp. 123-135, 1996.
- [61] B. Lengsfeld and D. R. Yarkony, "Nonadiabatic interactions between potential energy surfaces: Theory and applications," vol. 82, no. 2, pp. 1-71, 1992.
- [62] P. Politzer and J. S. Murray, "The fundamental nature and role of the electrostatic potential in atoms and molecules," vol. 108, no. 3, pp. 134-142, 2002.
- [63] F. Weinhold, C. Landis, and E. Glendening, "What is NBO analysis and how is it useful?," vol. 35, no. 3, pp. 399-440, 2016.
- [64] Y. Ekincioglu, H. Ş. Kılıç, and Ö. Dereli, "Structural Parameters, Electronic, Spectroscopic and Nonlinear Optical Theoretical Research of 1-(m-Chlorophenyl) piperazine (mCPP) Molecule," vol. 4, no. 2, pp. 88-97.

- [65] K. Andersson, P. A. Malmqvist, B. O. Roos, A. J. Sadlej, and K. Wolinski, "Second-order perturbation theory with a CASSCF reference function," vol. 94, no. 14, pp. 5483-5488, 1990.
- [66] J. A. Agwupuye, H. Louis, T. O. Unimuke, P. David, E. I. Ubana, and Y. L. Moshood, "Electronic structure investigation of the stability, reactivity, NBO analysis, thermodynamics, and the nature of the interactions in methyl-substituted imidazolium-based ionic liquids," vol. 337, p. 116458, 2021.
- [67] M. Lillo-Ródenas, D. Cazorla-Amorós, and A. Linares-Solano, "Understanding chemical reactions between carbons and NaOH and KOH: an insight into the chemical activation mechanism," vol. 41, no. 2, pp. 267-275, 2003.
- [68] A. Kepceoglu, Y. Gundogdu, O. Dereli, and H. S. Kilic, "Molecular Structure and TD-DFT Study of the Xylene Isomers," *Gazi University Journal of Science*, vol. 32, no. 1, pp. 300-308, 2019.
- [69] A. Kepceoğlu, N. Köklü, Y. Gündoğdu, Ö. Dereli, and H. Kilic, "Analysis of the xylenol isomers by femtosecond laser time of flight mass spectrometry," *Canadian Journal of Physics*, vol. 96, no. 7, pp. 711-715, 2018.